Pillar[5]arene-based dually crosslinked supramolecular gel as a sensor for the detection of adiponitrile

Maksim Rodin, David Helle, Dirk Kuckling*
Paderborn University, Warburger Str. 100, 33098 Paderborn, Germany

Supporting Information

Synthetic procedures

Precursor synthesis

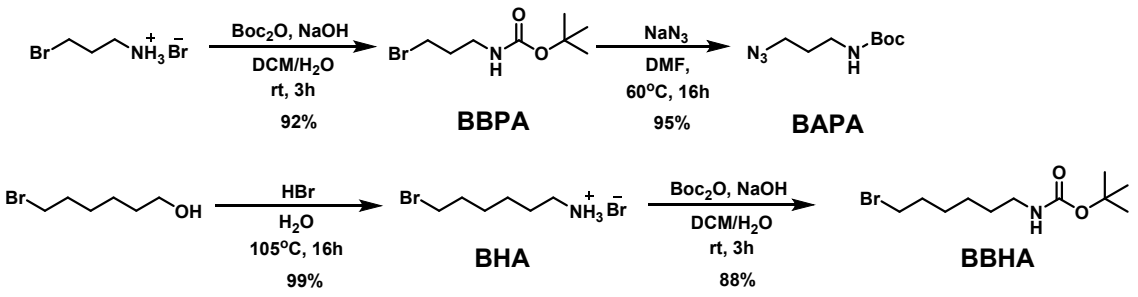

Synthesis of tert-butyl (3-bromopropyl)carbamate (BBPA)

The procedure was adapted from [S1].

In a 1000 ml round-bottom flask a solution of 5.6 g (25.7 mmol) di-*tert*-butyl dicarbonate in 200 ml DCM was mixed with a solution of 8.5 g (38.8 mmol) 3-bromopropylamine hydrobromide in 100 ml H_2O at vigorous stirring. To the mixture 40 ml 2 M NaOH solution were added dropwise over 15 min. After stirring for 3 h the organic phase was separated and washed with 100 ml 1 M HCl solution and 100 ml brine, then dried over $MgSO_4$ and the solvent was evaporated *in vacuo*. The crude product (yellow oil) was recrystallized from iso-hexane. BBPA was obtained as white needle-like crystals (5.6503 g; 23.7 mmol; 92 %).

T_{mp} = 37.6 °C (Lit.: 36–38 °C[S2]).

^{1}H NMR (700 MHz, $CDCl_3$) δ (ppm) = 4.68 (br s, 1H, N**H**), 3.43 (tr, $^3J_{HH}$ = 6.5 Hz, 2H, Br-C**H**$_2$), 3.26 (m, 2H, NH-C**H**$_2$), 2.04 (quint, $^3J_{HH}$ = 6.3 Hz, 2H, NH-CH$_2$-C**H**$_2$), 1.43 (s, 9H, C**H**$_3$).

^{13}C NMR (176 MHz, $CDCl_3$) δ (ppm) = 156.2 (**C**=O), 79.6 (**C**(CH$_3$)$_3$), 39.2 (NH-**C**H$_2$), 32.9 (NH-CH$_2$-**C**H$_2$), 31.0 (Br-**C**H$_2$), 28.6 (**C**H$_3$).

ESI-MS: cacld for [*M* + Na]$^+$ *m/z* = 260.0262, found *m/z* = 260.0254.

Synthesis of tert-butyl (3-azidopropyl)carbamate (BAPA)

In a 100 ml three-necked flask 0.286 g (4.4 mmol) NaN_3 were dissolved in 15 ml anhydrous DMF und Ar flow. To the solution 1.0 g (4.2 mmol) BAPA in 5 ml DMF were added and the reaction mixture was stirred at 70 °C for 24 h. After the reaction was complete, 20 ml H_2O and 20 ml ethyl acetate were added to the mixture. The phases were separated, and the aqueous phase was extracted with 20 ml EtOAc, then the combined organic phases were washed with H_2O (3×40 ml), dried over $MgSO_4$, and the solvent was carefully evaporated in vacuo. BAPA was obtained as a yellow viscous liquid (0.7503 g; 3.75 mmol; 89 %).

^{1}H NMR (700 MHz, $CDCl_3$) δ (ppm) = 4.66 (br s, 1H, N**H**), 3.35 (tr, $^{3}J_{HH}$ = 6.7 Hz, 2H, N_3-C**H**$_2$), 3.20 (m, 2H, NH-C**H**$_2$), 1.76 (quint, $^{3}J_{HH}$ = 6.6 Hz, 2H, NH-CH_2-C**H**$_2$), 1.44 (s, 9H, C**H**$_3$).
^{13}C NMR (176 MHz, $CDCl_3$) δ (ppm) = 156.1 (**C**=O), 79.6 (**C**$(CH_3)_3$), 49.3 (N_3-**C**H_2), 38.2 (NH-**C**H_2), 29.5 (NH-CH_2-**C**H_2), 28.6 (**C**H_3).
ESI-MS: cacld for [*M* + Na]$^+$ *m/z* = 223.1171, found *m/z* = 223.1152.

Synthesis of 6-bromohexan-1-amine hydrobromide (BHA)

The procedure was adapted from [S3].
3.05 g (25.6 mmol) 6-aminohexan-1-ol were dissolved in 30 ml 48 % HBr in H_2O. The mixture was heated up to 105 °C and refluxed for 16 h. After the reaction was complete, the solvent was removed *in vacuo* to give BHA as an ocher solid (6.62 g; 25.4 mmol; 99 %).

T_{mp} = 142 °C. (Lit.: 142–143 °C[S4]).
^{1}H NMR (700 MHz, D_2O) δ (ppm) = 3.55 (t, $^{3}J_{HH}$ = 6.7 Hz; 2H, Br-C**H**$_2$), 3.03 (m, 2H, NH_3^+-C**H**$_2$), 1.90 (m, 2H, Br-CH_2-C**H**$_2$), 1.70 (m, 2H, NH_3^+-CH_2-C**H**$_2$), 1.50 (m, 2H, Br-CH_2-CH_2-C**H**$_2$), 1.43 (m, 2H, NH_3^+-CH_2-CH_2-C**H**$_2$).
^{13}C NMR (176 MHz, D_2O) δ (ppm) = 39.5 (NH_3^+-**C**H_2), 35.0 (Br-**C**H_2), 31.8 (Br-CH_2-**C**H_2), 26.8 (Br-CH_2-CH_2-**C**H_2), 26.6 (NH_3^+-CH_2-**C**H_2), 24.7 (NH_3^+-CH_2-CH_2-**C**H_2).
ESI-MS: cacld for [*M* + H]$^+$ *m/z* = 180.0382, 182.0362, found *m/z* = 180.0400, 182.0382.

Synthesis of tert-butyl (6-bromohexyl)carbamate (BBHA)

BHA (2.47 g; 9.47 mmol) and Boc_2O (4.24 g; 19.43 mmol) were dissolved in 55 ml DCM To the mixture at vigorous stirring 40 ml 1 M NaOH in H_2O were added dropwise over 20 min. After reacting for 4 h at RT 50 ml water were added, then the organic phase was separated, dried over $MgSO_4$, and the solvent was evaporated *in vacuo*. The obtained crude product was purified by column chromatography (SiO_2; iso-hexane:EtOAc 10:0 to 10:1). BBHA (2.33 g; 8.32 mmol; 88 %) was obtained as slightly yellow oil.

^{1}H NMR (700 MHz, $CDCl_3$) δ (ppm) = 4.51 (br s, 1H, N**H**), 3.39 (t, $^{3}J_{HH}$ = 6.8 Hz; 2H, Br-C**H**$_2$), 3.10 (m, 2H, NH-C**H**$_2$), 1.85 (quint, $^{3}J_{HH}$ = 7.2 Hz; 2H, Br-CH_2-C**H**$_2$), 1.48 (m, 2H, NH-CH_2-C**H**$_2$), 1.46-1.40 (m, 11H, Br-CH_2-CH_2-C**H**$_2$ and C**H**$_3$), 1.33 (m, 2H, NH-CH_2-CH_2-C**H**$_2$).
^{13}C NMR (176 MHz, $CDCl_3$) δ (ppm) = 156.2 (**C**=O), 79.3 (**C**$(CH_3)_3$), 40.7 (NH-**C**H_2), 34.0 (Br-**C**H_2), 32.9 (Br-CH_2-**C**H_2), 30.1 (NH-CH_2-**C**H_2), 28.6 (**C**H_3), 28.0 (Br-CH_2-CH_2-**C**H_2), 26.1 (NH-CH_2-CH_2-**C**H_2).

ESI-MS: cacld for $[M + Na]^+$ *m/z* = 302.0732, 304.0711, found *m/z* = 302.0732, 304.0710.

Synthesis of VDMA[S5,S6]

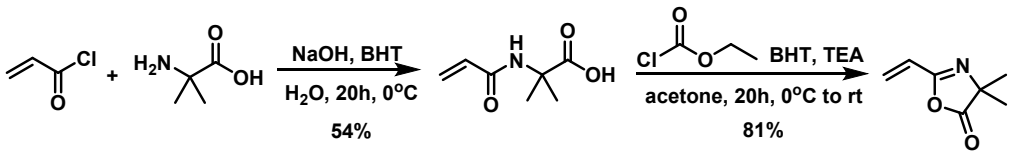

Synthesis of 2-acrylamido-2-methylpropanoic acid

In the solution of 8.85 g (0.22 mol) NaOH in 22 ml H_2O 25 mg (0.11 mmol) BHT and subsequently 10.0 g (0.097 mol) methyl alanine were dissolved. The solution was cooled down to 0 °C and 9 ml (0.11 mol) acryloyl chloride were added dropwise over 30 min. After stirring for 20 h 11.5 ml HCl (conc.) were added, and the mixture was stirred for additional 2 h. The white precipitate was isolated by filtration and washed with 0.1 M HCl on the frit followed by recrystallization from H_2O/EtOH (1:1, v/v). 2-acrylamido-2-methylpropanoic acid was obtained as a white solid (8.20 g; 52.2 mmol; 54%).

Tmp: 192 °C (Lit.: 202 °C[S5]; 196–197 °C[S7]).

^{1}H NMR (700 MHz; DMSO-d_6) δ (ppm) = 12.17 (br s, 1H, COO**H**); 8.24 (s, 1H, N**H**); 6.25 (dd, $^3J_{HH}$ = 17.1 Hz, $^3J_{HH}$ = 10.3 Hz; 1H, CH_2=C**H**); 6.05 (dd, $^3J_{HH}$ = 17.1 Hz, $^2J_{HH}$ = 2.2 Hz; 1H, C$\mathbf{H}_{cis}$); 5.57 (dd, $^3J_{HH}$ = 10.2 Hz, $^2J_{HH}$ = 2.2 Hz; 1H, C$\mathbf{H}_{trans}$); 1.36 (s, 6H, C$\mathbf{H}_3$).

^{13}C NMR (176 MHz; DMSO-d_6) δ (ppm) = 175.4 (**C**(O)OH); 163.8 (**C**(O)-NH); 131.6 (CH_2=**C**H); 125.3 (**C**H_2=CH); 54.8 (**C**$(CH_3)_2$); 24.9 (**C**H_3).

ESI-MS: cacld for $[M + Na]^+$ *m/z* = 180.0637, found *m/z* = 180.0626.

Synthesis of 2-vinyl-4,4-dimethyl azlactone (VDMA)

Under Ar atmosphere 4.0 g (25.5 mmol) 2-acrylamido-2-methylpropanoic acid and 18 mg (0.08 mmol) BHT were suspended in 80 ml acetone. The solid dissolved upon addition of 5.25 ml (38 mmol) triethylamine. The solution was stirred for 20 min and then cooled down to 0 °C followed by adding 2.5 ml (25.5 mmol) ethyl chloroformate dropwise over 20 min. The mixture was stirred for 3 h at 0 °C and then for additional 16 h at RT. Formation of a white precipitate was observed. The precipitate was filtered out and washed with acetone on the frit. The filtrate was evaporated, a white precipitate was formed again. To the residue 50 ml iso-hexane was added and

the filtration/evaporation cycle was repeated 3 times until no precipitate formation in the residue occurred. VDMA was obtained as colorless to slightly yellow oil (2.88 g; 20.7 mmol; 81%).

^{1}H NMR (700 MHz, $CDCl_3$) δ (ppm) = 6.32-6.20 (m, 2H, CH_2=C**H** and C$\mathbf{H}_{cis}$); 5.93 (dd, 1H, C$\mathbf{H}_{trans}$); 1.46 (s, 6H, C$\mathbf{H}_3$).
^{13}C NMR (176 MHz, $CDCl_3$) δ (ppm) = 180.9 (**C**=O); 159.2 (O-**C**=N); 129.2 (**C**H_2); 124.1 (**C**H); 65.9 (**C**$(CH_3)_2$); 24.8 (**C**H_3).
ESI-MS: cacld for $[M + H]^+$ *m/z* = 140.0712, found *m/z* = 140.0706.

Synthesis of the photo-crosslinker DMIEA[S8,S9]

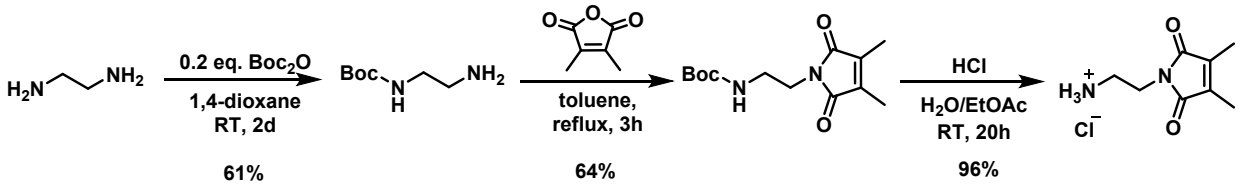

Synthesis of tert-butyl (2-aminoethyl)carbamate (EDA-Boc)
In a 1000 ml flask with an attached $CaCl_2$ tube 33.3 ml (0.5 mol) ethylene diamine were dissolved in 200 ml 1,4-dioxane and to the mixture a solution of 21.92 g (0.1 mol) di-*tert*-butyl dicarbonate in 200 ml 1,4-dioxane was dropwise added over 3 h. After 2 d the mixture was filtered, and the filtrate was evaporated. To the yellow oily residue 300 ml water were added, which lead to the formation of a white precipitate. After it was removed by filtration, the filtrate was saturated with NaCl, and the formed precipitate was filtered out as well. The yellow solution was extracted with DCM (8×100 ml). The combined organic phases were dried over $MgSO_4$, and the DCM was evaporated to obtain *tert*-butyl (2-aminoethyl)carbamate as a yellow oil (9.73 g; 60.7 mmol; 61 %).

^{1}H NMR (700 MHz, $CDCl_3$) δ (ppm) = 4.94 (br s, 1H, N**H**); 3.17 (br q, 2H, C$\mathbf{H}_2$-NH), 2.79 (t, $^3J_{HH}$ = 5.9 Hz; 2H, C$\mathbf{H}_2$-NH_2); 1.43 (s, 6H, C$\mathbf{H}_3$)
^{13}C NMR (176 MHz, $CDCl_3$) δ (ppm) = 156.4 (**C**=O); 79.4 (**C**$(CH_3)_3$); 43.5 (**C**H_2-NH); 42.0 (**C**H_2-NH_2); 28.6 (**C**H_3).
ESI-MS: cacld for $[M + Na]^+$ *m/z* = 161.1402, found *m/z* = 161.1394.

Synthesis of tert-butyl (2-(3,4-dimethyl-2,5-dioxo-2,5-dihydro-1H-pyrrol-1-yl)ethyl)carbamate (DMIEA-Boc)

In a 500 ml round-bottom flask equipped with a Dean–Stark apparatus and a reflux 2,3-dimethylmaleic anhydride (7.06 g; 56 mmol) was dissolved in 200 ml toluene. As the mixture was heated up to 130 °C, a solution of EDA-Boc (9.00 g; 56 mmol) in 70 ml toluene was dropwise added within 15 min. After reacting under reflux for 4 h the mixture became orange, the heating was stopped, and the solvent was evaporated. The crude product (orange oil) was dissolved in 30 ml $CHCl_3$ and precipitated into cooled (acetone/N_2 bath) pentane. The solid was collected by filtration and the precipitation was repeated once again. After drying *in vacuo* DMIEA-Boc (9.589 g; 35.74 mmol; 64 %) was obtained as brownish solid.

Tmp: 108.5 °C (Lit. 106 °C[S9])

^{1}H NMR (700 MHz, $CDCl_3$) δ (ppm) = 4.81 (br s, 1H, N**H**); 3.60 (t, $^3J_{HH}$ = 5.5 Hz; 2H, C**H**$_2$-N); 3.30 (br q, 2H, C**H**$_2$-NH); 1.95 (s, 6H, C(C**H**$_3$)=C(C**H**$_3$)); 1.39 (C(C**H**$_3$)$_3$).

^{13}C NMR (176 MHz, $CDCl_3$) δ (ppm) = 172.4 (N-**C**=O); 156.1 (**C**(=O)-NH); 137.5 (**C**(CH$_3$)=**C**(CH$_3$)); 79.5 (**C**(CH$_3$)$_3$); 40.0 (**C**H$_2$-NH); 38.2 (**C**H$_2$-N); 28.5 (C(**C**H$_3$)$_3$); 8.9 (C(**C**H$_3$)=C(**C**H$_3$)).

ESI-MS: cacld for $[M + Na]^+$ *m/z* = 291.1321, found *m/z* = 291.1311.

Synthesis of 1-(2-aminoethyl)-3,4-dimethyl-1H-pyrrole-2,5-dione (DMIEA)

In a 250 ml round-bottom flask 9.0 g DMIEA-Boc were suspended in 100 ml ethyl acetate, and to the mixture 6.5 ml HCl (conc.) were added dropwise over 15 min. After 19 h a brownish precipitate formed was collected by filtration. The filtrate was turbid; therefore, it was filtered once again. Both solid fractions were combined and dried *in vacuo*. DMIEA (6.603 g; 32.26 mmol; 96 %) was obtained as a brownish solid.

Tmp: 209–211 °C (decomposition). (Lit. 210 °C[S9])

^{1}H NMR (700 MHz, DMSO-d_6) δ (ppm) = 8.20 (br s, 3H, N**H**$_3^+$); 3.65 (t, $^3J_{HH}$ = 6.2 Hz; 2H, C**H**$_2$-N); 2.93 (m, 2H, C**H**$_2$-NH$_3^+$); 1.90 (s, 6H, C**H**$_3$).

^{13}C NMR (176 MHz, DMSO-d_6) δ (ppm) = 171.6 (**C**=O); 136.9 (**C**(CH$_3$)); 37.3 (**C**H$_2$-NH$_3^+$); 35.0 (**C**H$_2$-N); 8.5 (**C**H$_3$).

ESI-MS: cacld for $[M]^+$ *m/z* = 169.0972, found *m/z* = 169.0975.

Synthesis of adhesion promoter[S8]

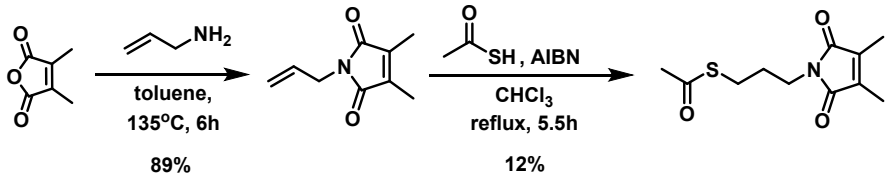

Synthesis of 1-allyl-3,4-dimethyl-1H-pyrrole-2,5-dione (ADMI)

15 ml (200 mmol) allyl amine were added to the solution of 2,3-dimethylmaleic anhydride (5.00 g; 39.65 mmol) in 50 ml toluene in a 150 ml three-necked flask equipped with a Dean–Stark apparatus and a reflux. The reaction mixture was heated up to 135 °C and stirred for 6 h. Further, the solvent was removed by evaporation and the crude product (yellow oil) was purified by column chromatography (SiO_2; EtOAc:*iso*-hexane 1:2; $R_f = 0.9$). ADMI (5.805 g; 35.14 mmol; 89 %) was obtained as a colorless liquid.

^{1}H NMR (700 MHz, $CDCl_3$) δ (ppm) = 5.79 (ddt, $^3J_{HH}$ = 17.1 Hz, $^3J_{HH}$ = 10.2 Hz, $^3J_{HH}$ = 5.6 Hz; 1H, CH_2=C**H**); 5.16 (ddt, $^2J_{HH}$ = 1.6 Hz, $^3J_{HH}$ = 17.2 Hz, $^4J_{HH}$ = 1.4 Hz; 1H, C$\mathbf{H}_{cis}$); 5.13 (ddt, $^2J_{HH}$ = 1.3 Hz, $^3J_{HH}$ = 10.3 Hz, $^4J_{HH}$ = 1.3 Hz; 1H, C$\mathbf{H}_{trans}$); 4.08 (dt, $^2J_{HH}$ = 1.5 Hz, $^3J_{HH}$ = 5.6 Hz; 2H, C$\mathbf{H}_2$-N); 1.96 (s, 6H, C$\mathbf{H}_3$).

^{13}C NMR (176 MHz, $CDCl_3$) δ (ppm) = 172.0 (**C**=O); 137.4 (**C**(CH_3)); 132.2 (CH_2=**C**H); 117.5 (**C**H_2=CH); 40.2 (**C**H_2-N); 8.9 (**C**H_3).

ESI-MS: cacld for $[M + H]^+$ *m/z* = 166.0868, found *m/z* = 166.0854; cacld for $[M + Na]^+$ *m/z* = 188.0687, found *m/z* = 188.0676.

Synthesis of S-(3-(3,4-dimethyl-2,5-dioxo-2,5-dihydro-1H-pyrrol-1-yl)propyl) ethanethioate (DMIPTA)

In a 100 ml round-bottom flask ADMI (2.50 g; 15.13 mmol), AIBN (0.15 g; 0.91 mmol) and thioacetic acid (1.62 ml; 23.0 mmol) were dissolved in 15 ml $CHCl_3$. The solution was purged with Ar for 30 min followed by stirring at reflux for 5.5 h. Further, the mixture was washed with 25 ml saturated Na_2CO_3 solution and the aqueous phase was extracted with petroleum ether (2×45 ml). The combined organic phases were washed with brine (80 ml) and dried over $MgSO_4$. After evaporation of the solvent *in vacuo* the crude product was purified by column chromatography (SiO_2; EtOAc:*iso*-hexane 1:15; $R_f = 0.1$). DMIPTA (0.43 g; 1.77 mmol; 12 %) was obtained as an orange liquid.

^{1}H NMR (700 MHz, $CDCl_3$) δ (ppm) = 3.53 (t, $^{3}J_{HH}$ = 7.0 Hz; 2H, C**H**$_2$-N); 2.82 (t, $^{3}J_{HH}$ = 7.3 Hz; 2H, C**H**$_2$-S); 2.30 (s, 3H, C**H**$_3$-CO); 1.94 (s, 6H, C(C**H**$_3$)); 1.84 (quint, $^{3}J_{HH}$ = 7.0 Hz; 2H, CH_2-C**H**$_2$-CH_2).

^{13}C NMR (176 MHz, $CDCl_3$) δ (ppm) = 195.7 (**C**(=O)-S); 172.3 (**C**(=O)-N); 137.4 (**C**(CH_3)); 36.9 (**C**H_2-N); 30.8 (**C**H_3-CO); 28.9 (CH_2-**C**H_2-CH_2); 26.5 (**C**H_2-S); 8.9 (C(**C**H_3)).

ESI-MS: cacld for $[M + Na]^+$ *m/z* = 264.0670, found *m/z* = 264.0657.

Synthesis of DMIEA-modified p(DMAAm-co-VDMA) (PPC)

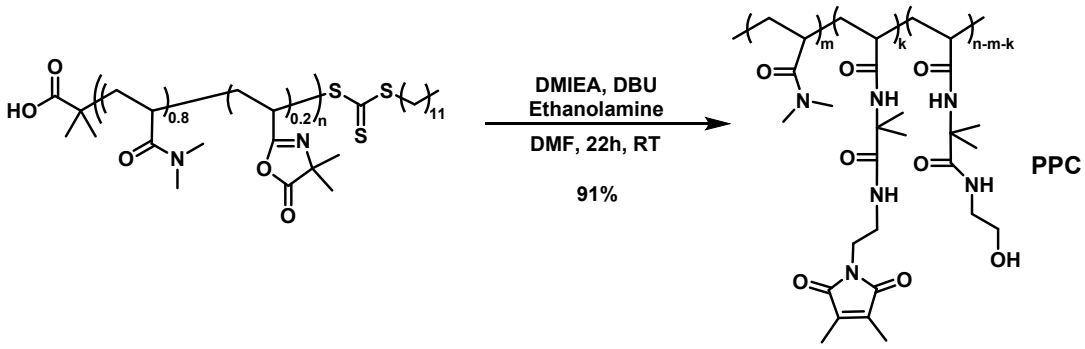

0.300 g poly(DMAAm-*co*-VDMA) dissolved in 5 ml DMF was mixed with a solution of DMIEA (0.108 g; 0.528 mmol) and DBU (0.095 g; 0.624 mmol) in 3 ml DMF in a pear-shaped flask. The reaction mixture was stirred at RT for 22 h followed by addition of 0.12 ml (1.90 mmol) ethanolamine and subsequent stirring for 1 h. The mixture was precipitated into 100 ml Et_2O at RT and the precipitate isolated by filtration. The crude product was resolved in 20 ml water, the solution was dialyzed in water for 72 h, and freeze-dried to obtain PPC (0.3547 g; 91 %) as a white solid.

^{1}H NMR (500 MHz, D_2O) δ (ppm) = 3.63 (br, 2H, $C_6H_6NO_2$-C**H**$_2$), 3.26–2.83 (m, 35H, N(CH_3)$_2$ and $C_6H_6NO_2$-CH_2-C**H**$_2$); 2.83–2.36 (m, 6H, backbone C**H**); 1.96 (s, 6H, C(C**H**$_3$)=C(C**H**$_3$)); 1.89–0.95 (m, 23H, backbone C**H**$_2$, C(=O)-NH-C(C**H**$_3$)$_2$).

SEC: M_n = 92700, *Đ* = 4.45.

NMR spectra of host and guest moieties

All the spectra are recorded on Bruker Ascent 700 spectrometer. Peaks of a deuterated solvent, water, and residual solvent marked with black, blue, and green circles, respectively.

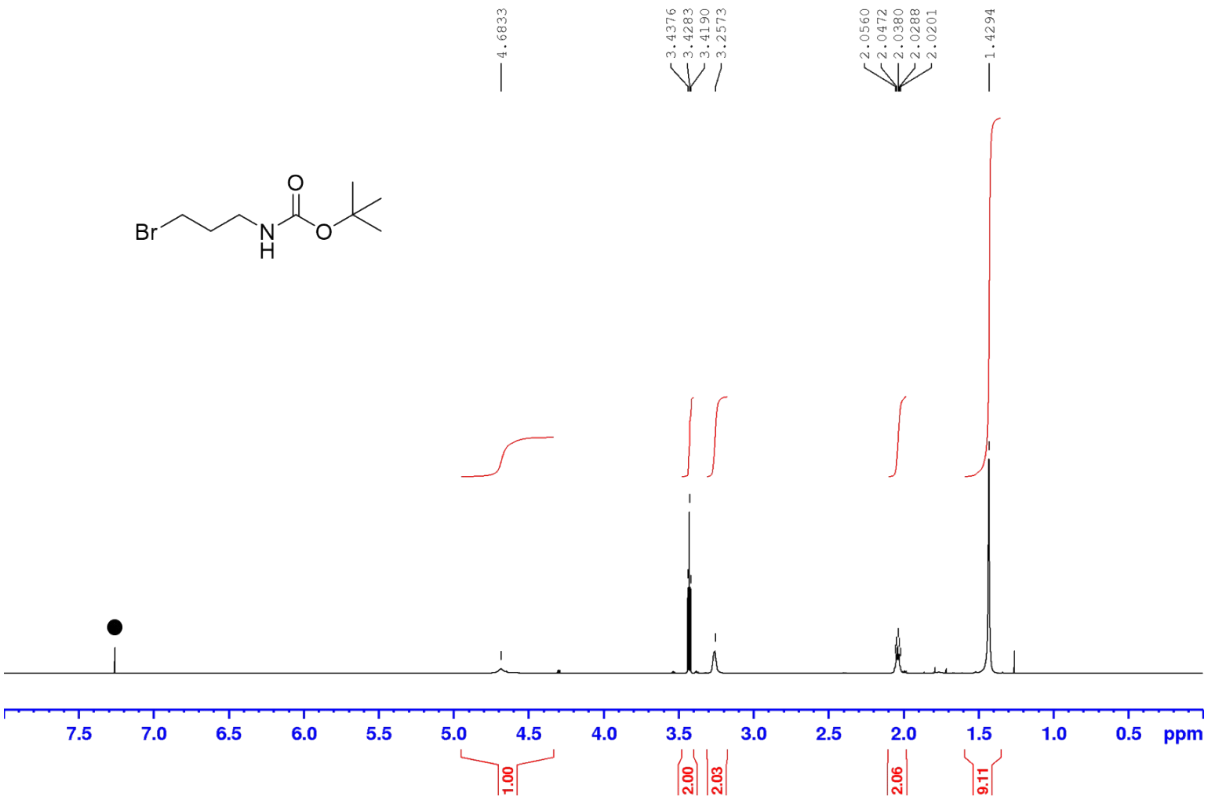

Figure S1. ^{1}H NMR spectrum of BBPA in $CDCl_3$.

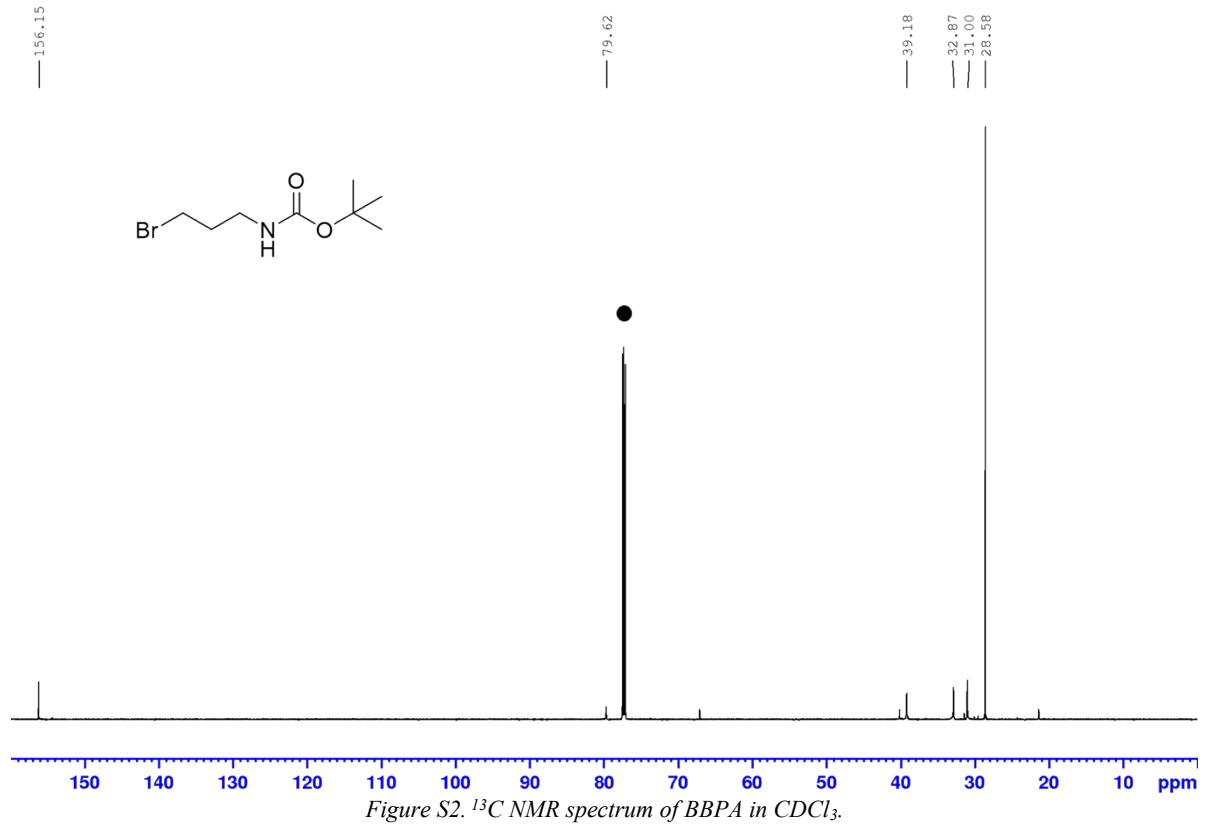

Figure S2. ^{13}C NMR spectrum of BBPA in $CDCl_3$.

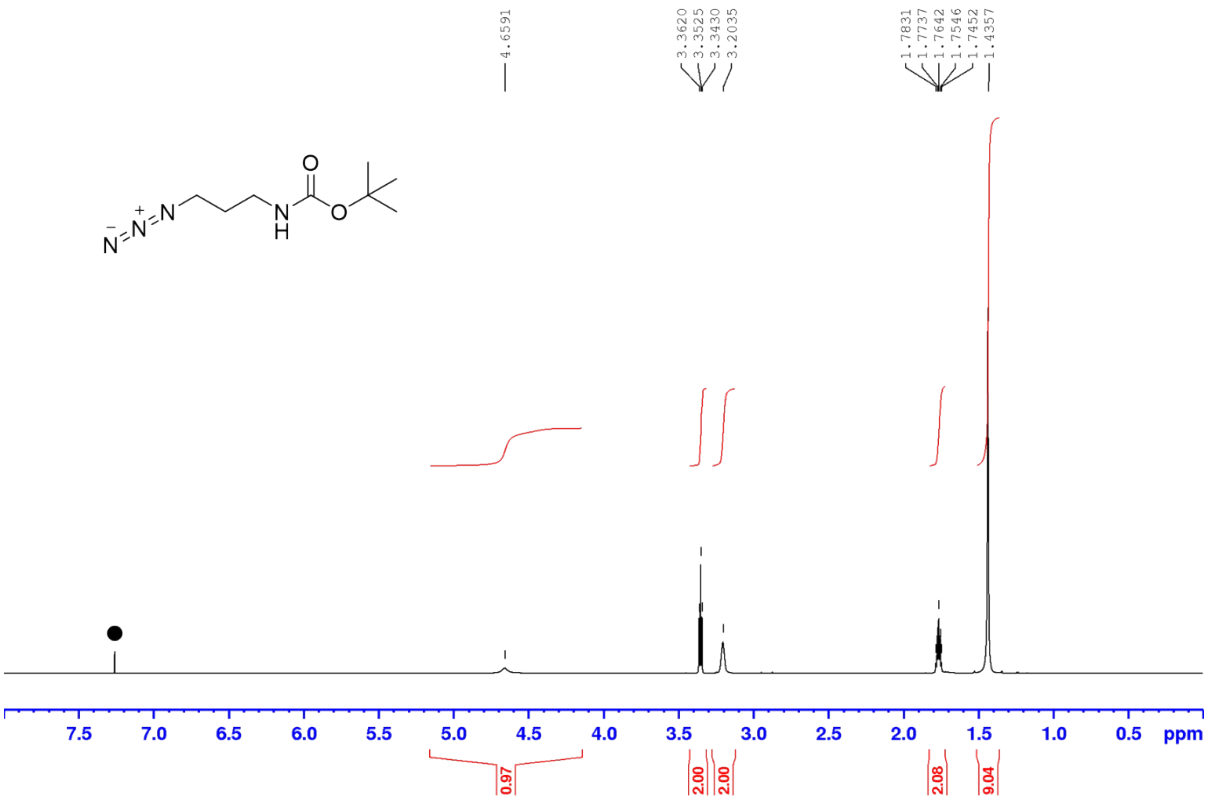

Figure S3. ^{1}H NMR spectrum of BAPA in $CDCl_3$.

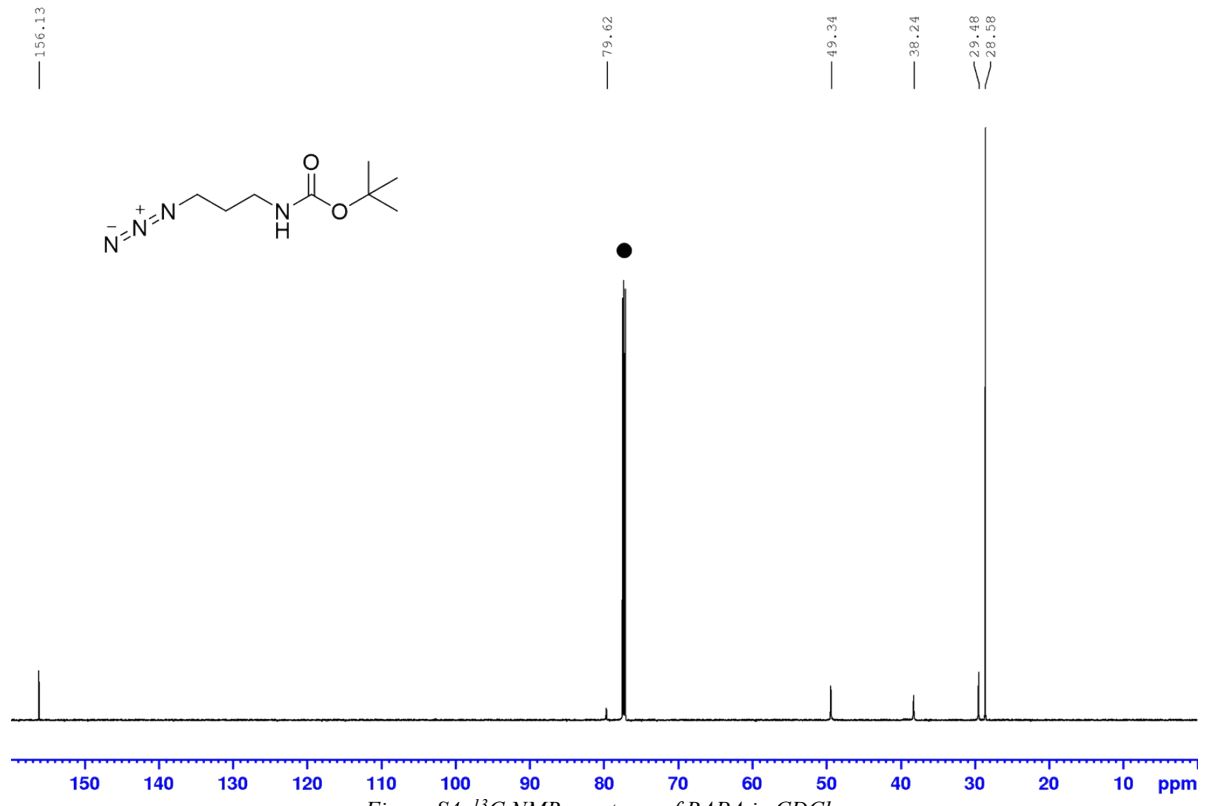

Figure S4. ^{13}C NMR spectrum of BAPA in $CDCl_3$.

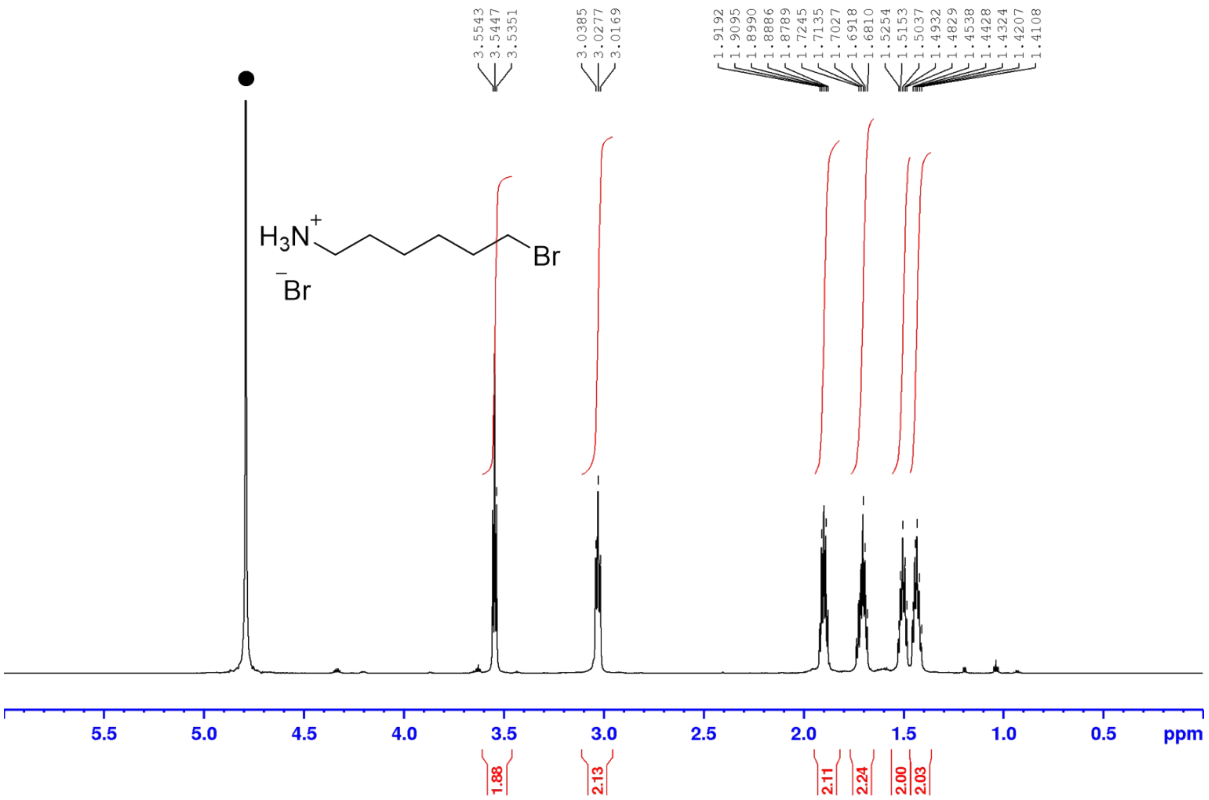

Figure S5. ^{1}H NMR spectrum of BHA in D_2O.

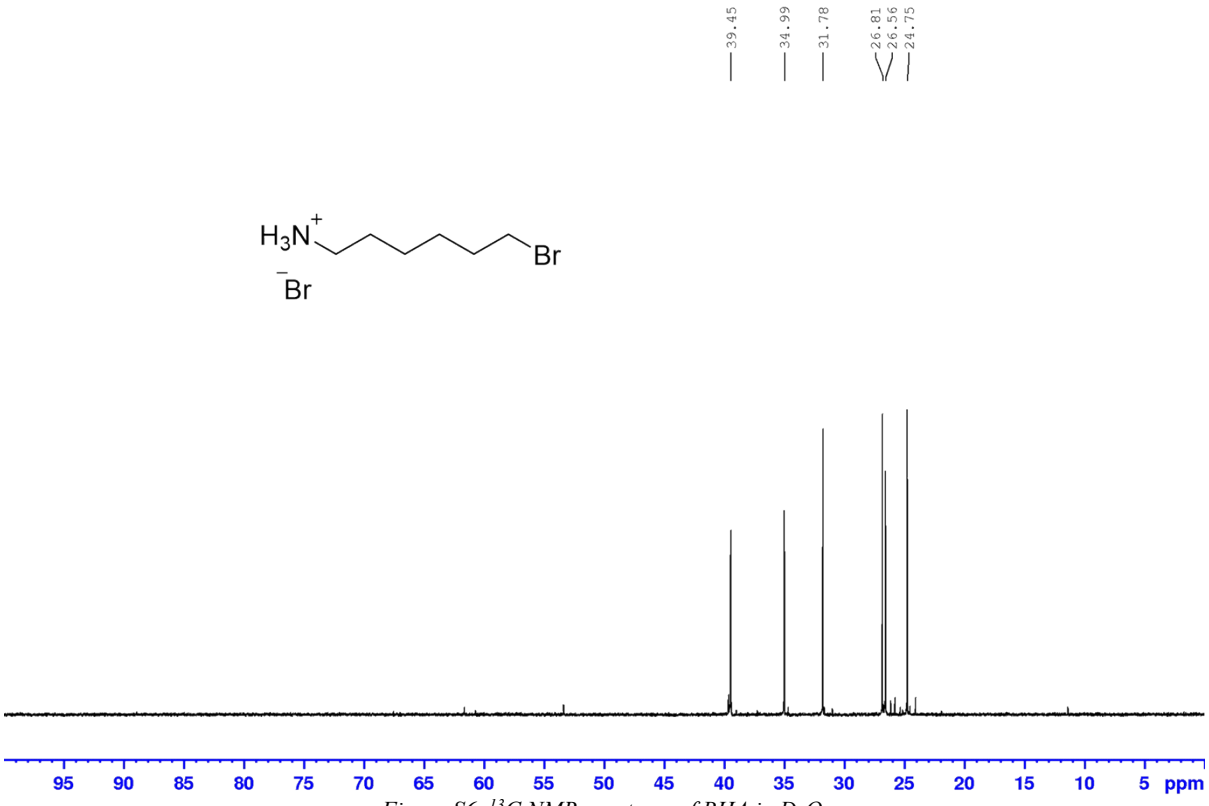

Figure S6. ^{13}C NMR spectrum of BHA in D_2O.

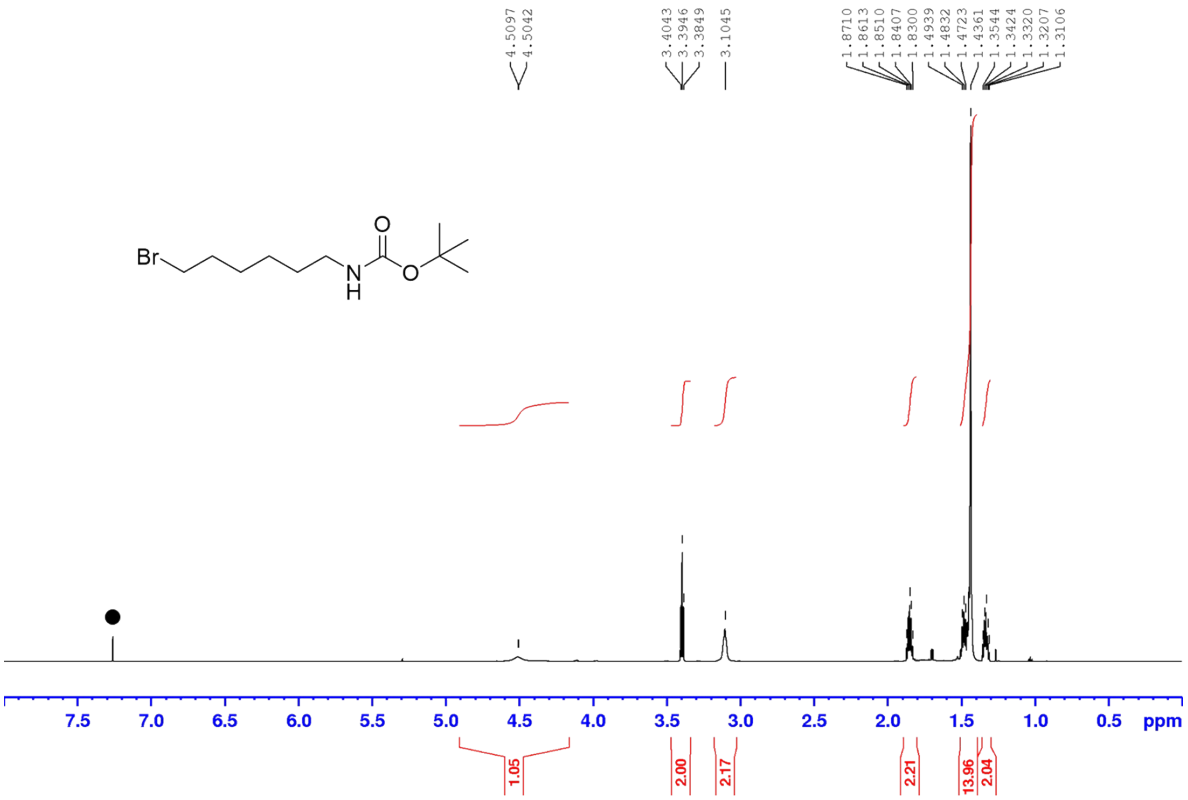

Figure S7. ^{1}H NMR spectrum of BBHA in $CDCl_3$.

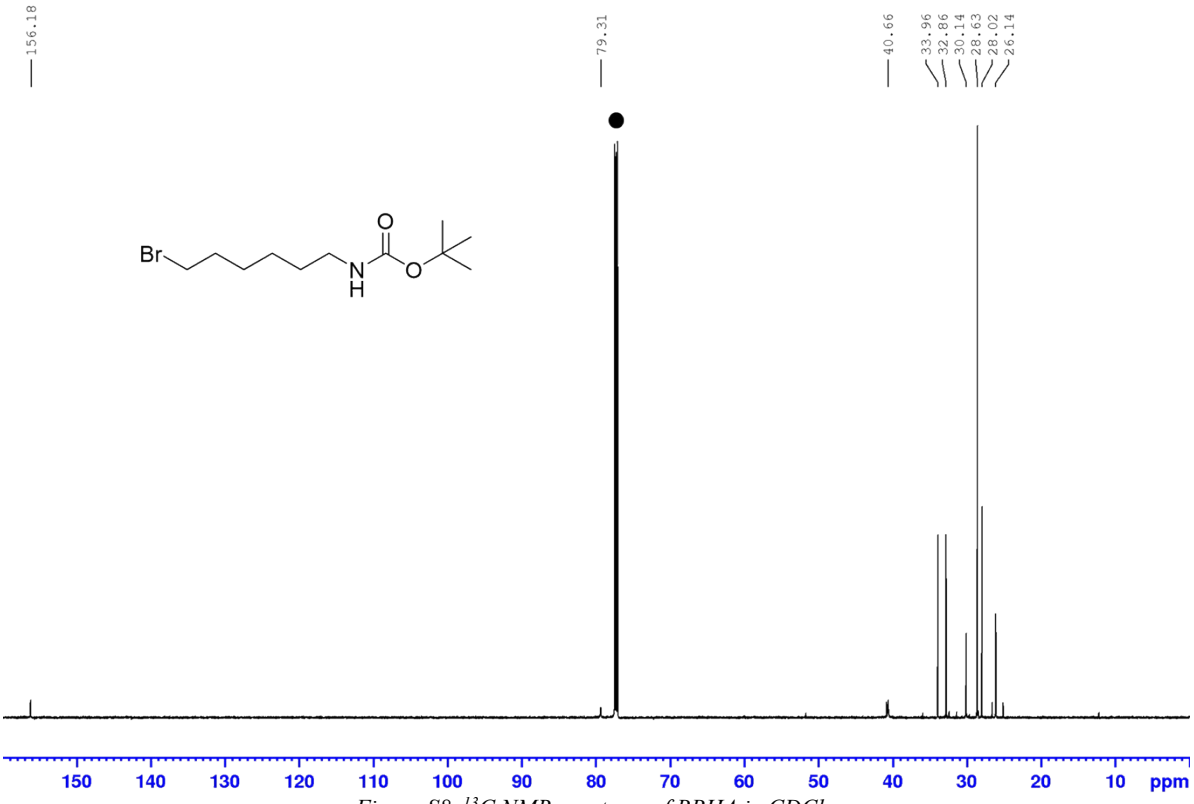

Figure S8. ^{13}C NMR spectrum of BBHA in $CDCl_3$.

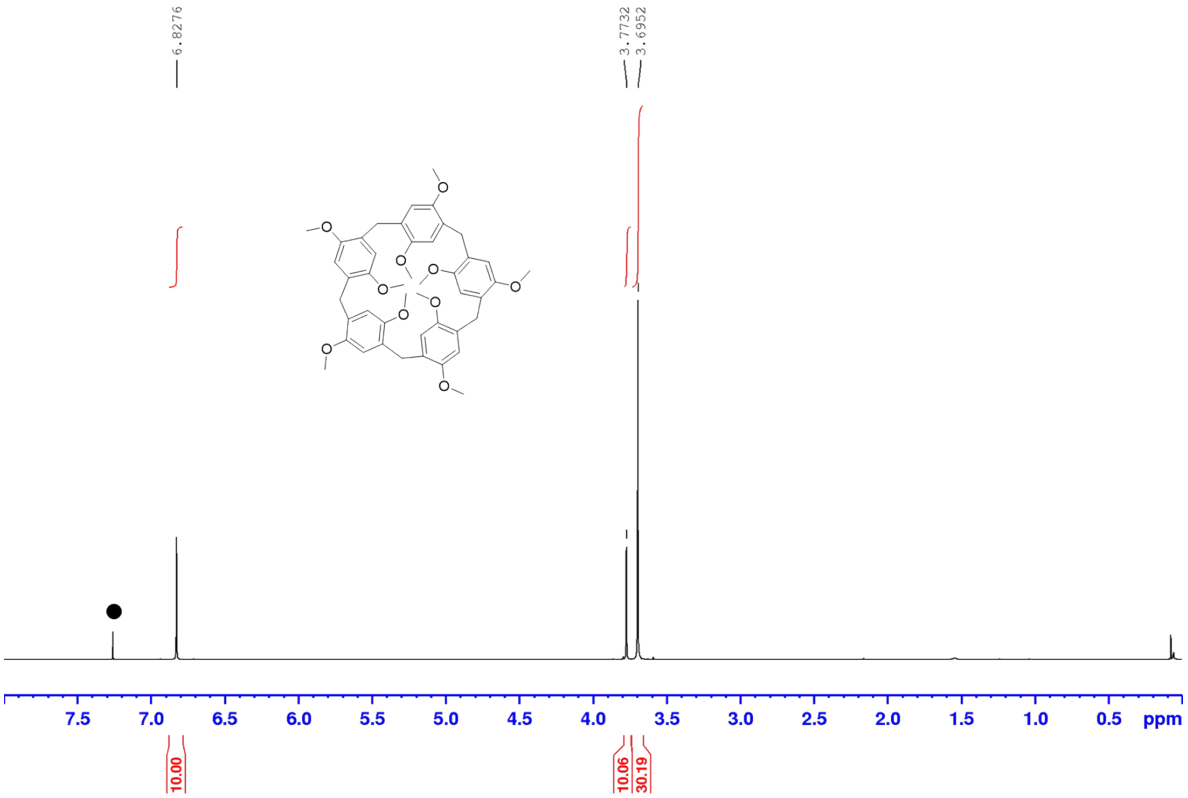

Figure S9. ^{1}H NMR spectrum of P5A in $CDCl_3$.

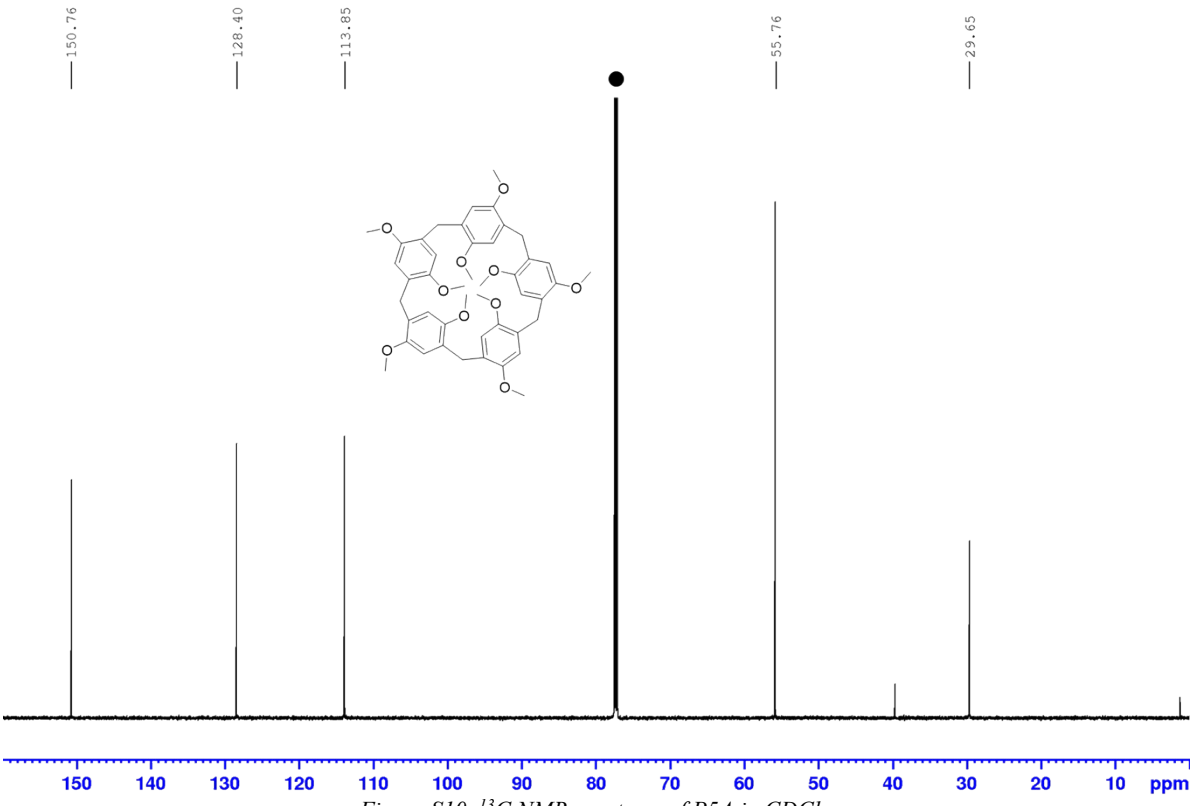

Figure S10. ^{13}C NMR spectrum of P5A in $CDCl_3$.

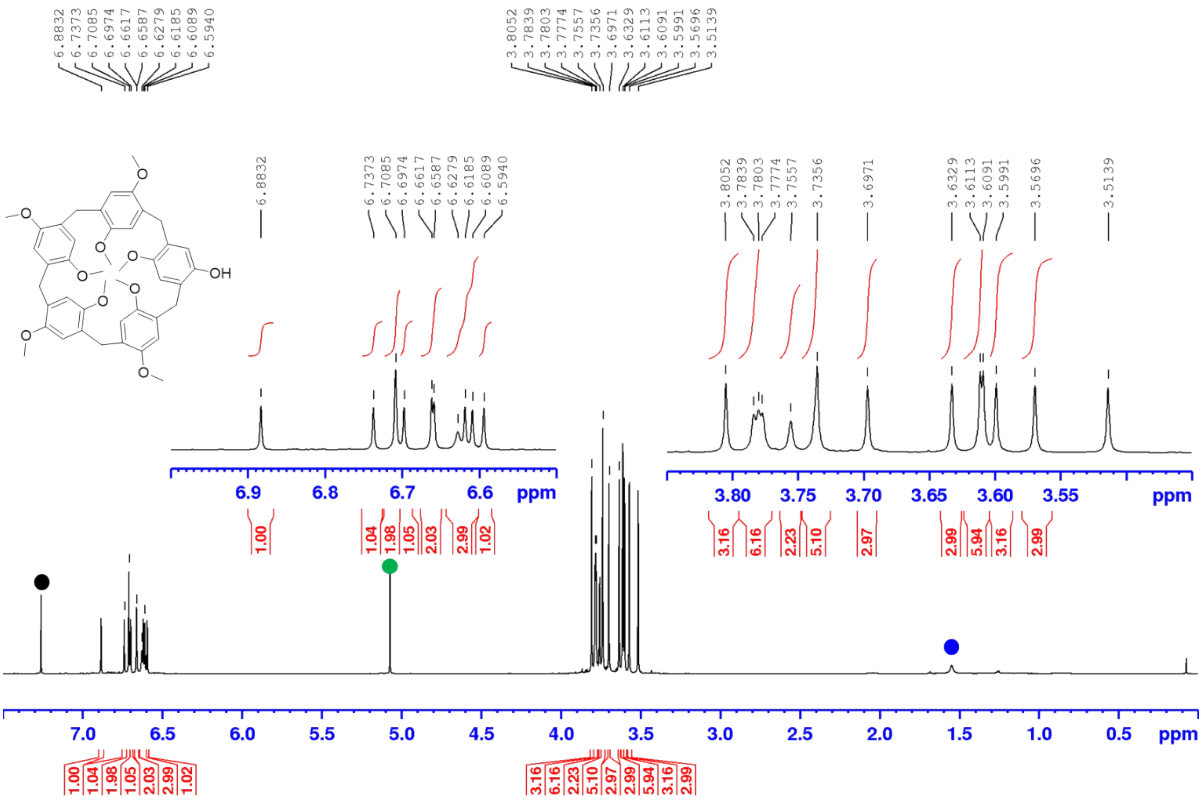

Figure S11. ^{1}H NMR spectrum of P5AOH in $CDCl_3$.

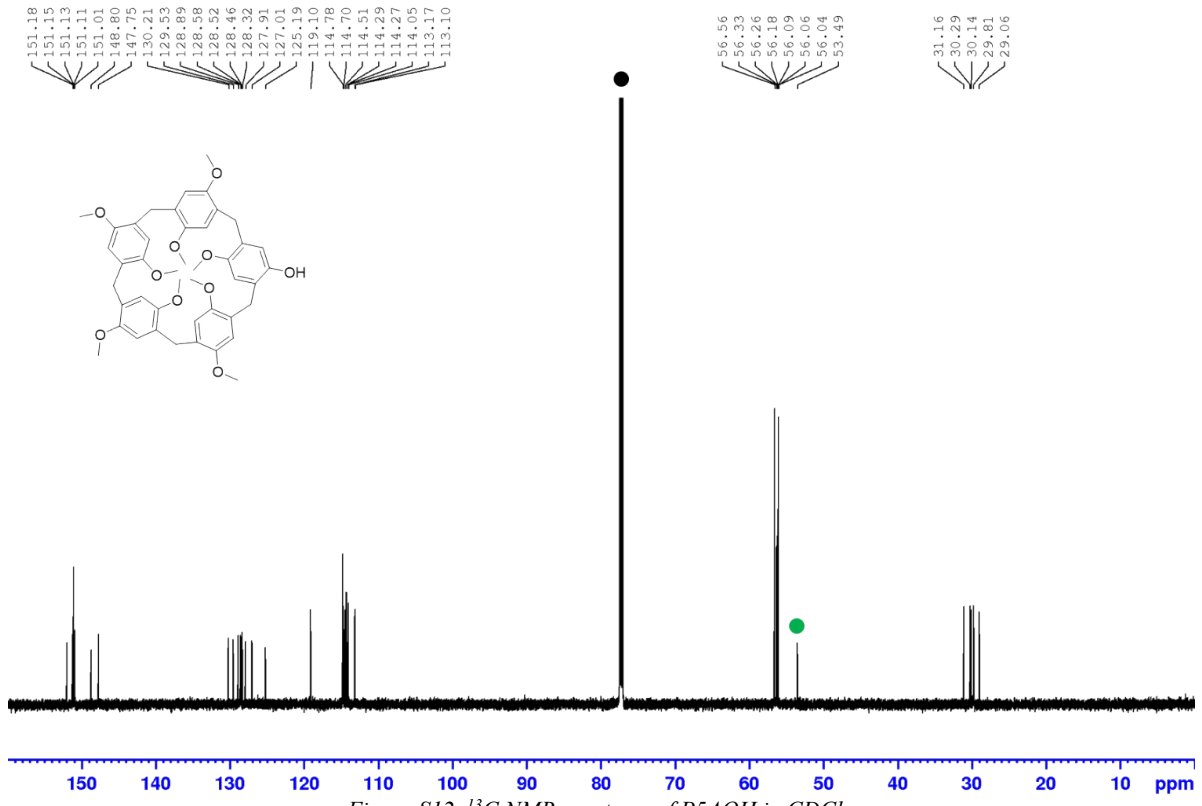

Figure S12. ^{13}C NMR spectrum of P5AOH in $CDCl_3$.

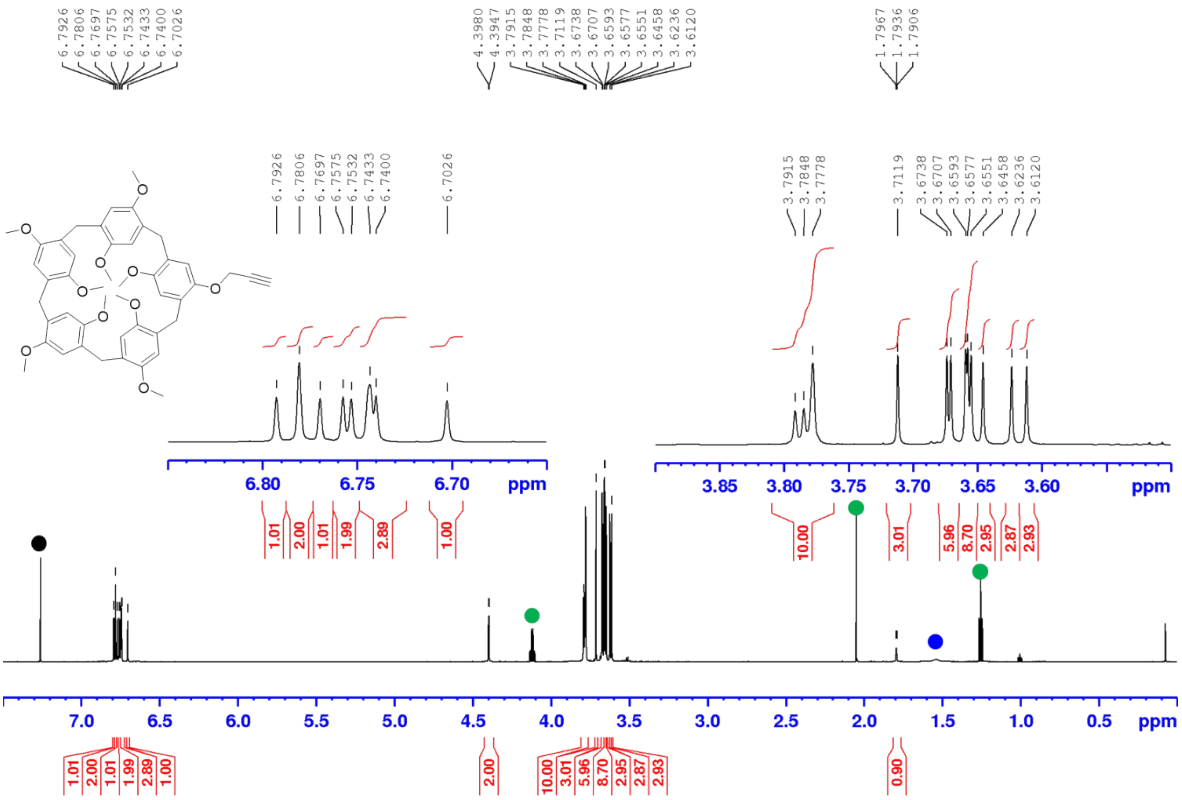

Figure S13. ^{1}H NMR spectrum of P5APR in $CDCl_3$.

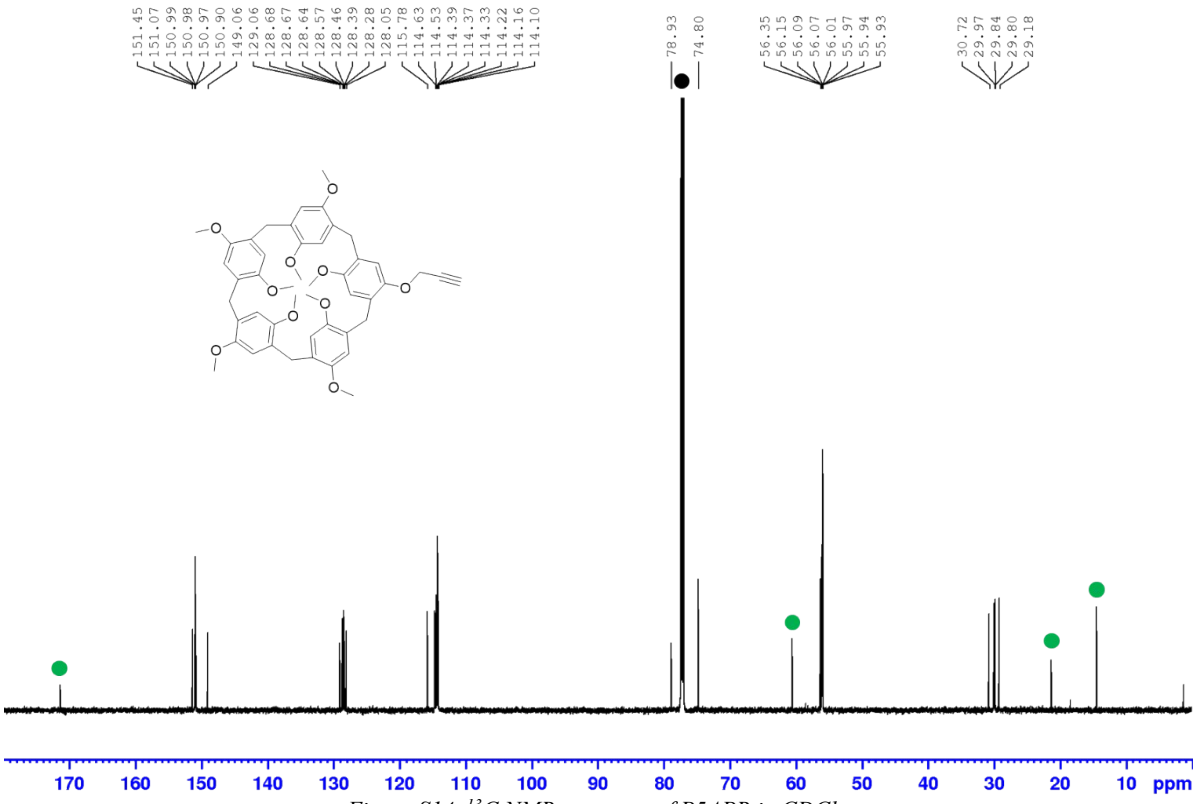

Figure S14. ^{13}C NMR spectrum of P5APR in $CDCl_3$.

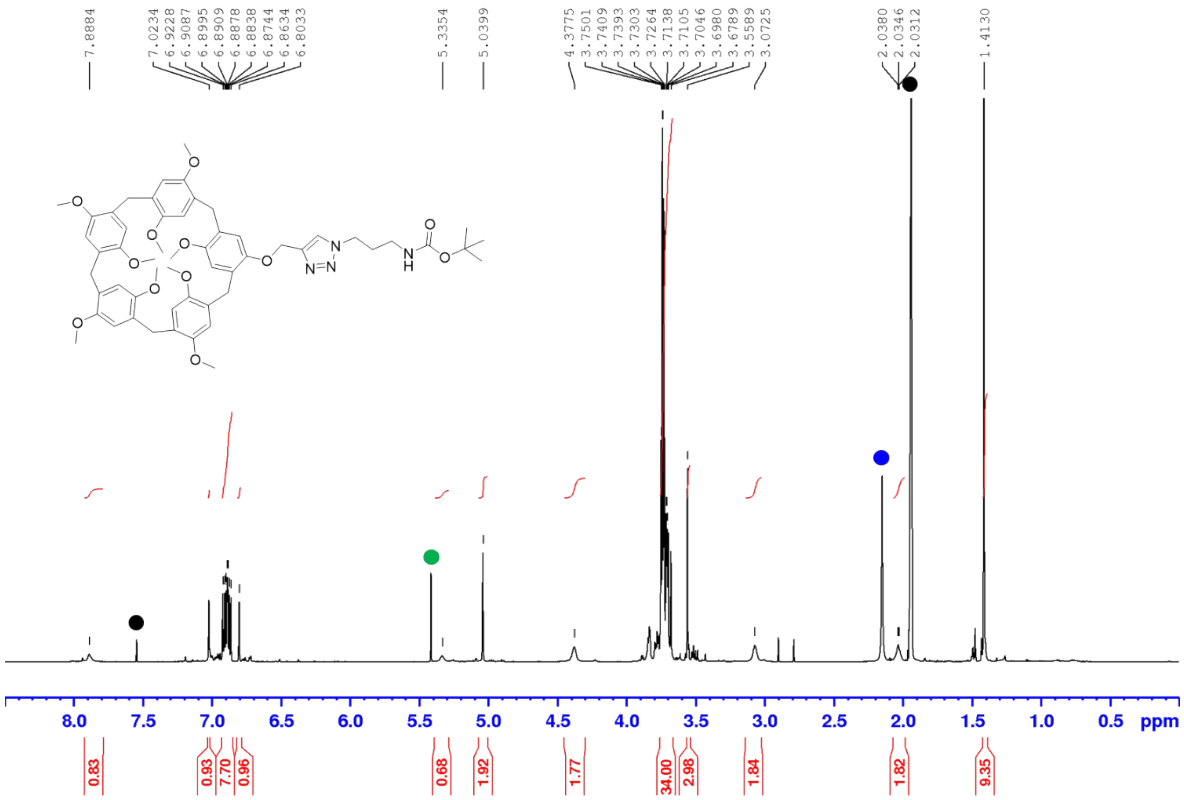

Figure S15. ^{1}H NMR spectrum of HT-Boc in $CDCl_3$: CD_3CN (1:3).

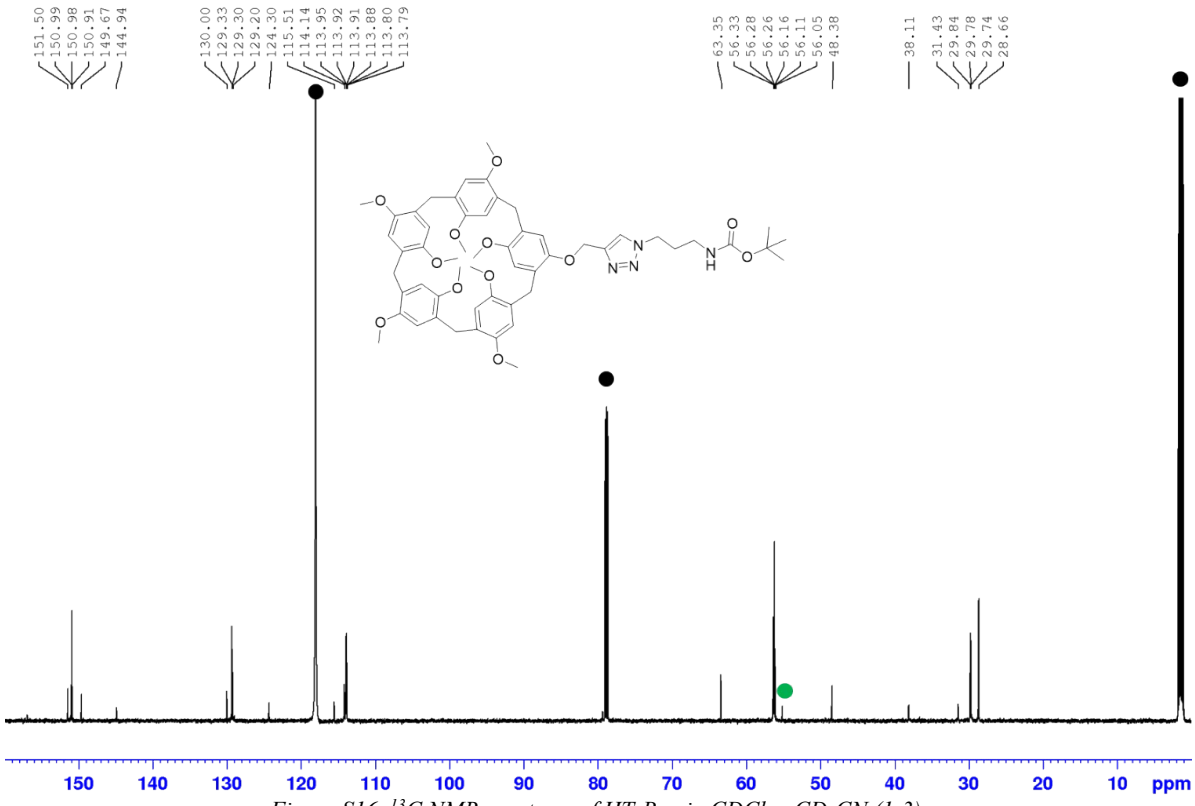

Figure S16. ^{13}C NMR spectrum of HT-Boc in $CDCl_3$: CD_3CN (1:3).

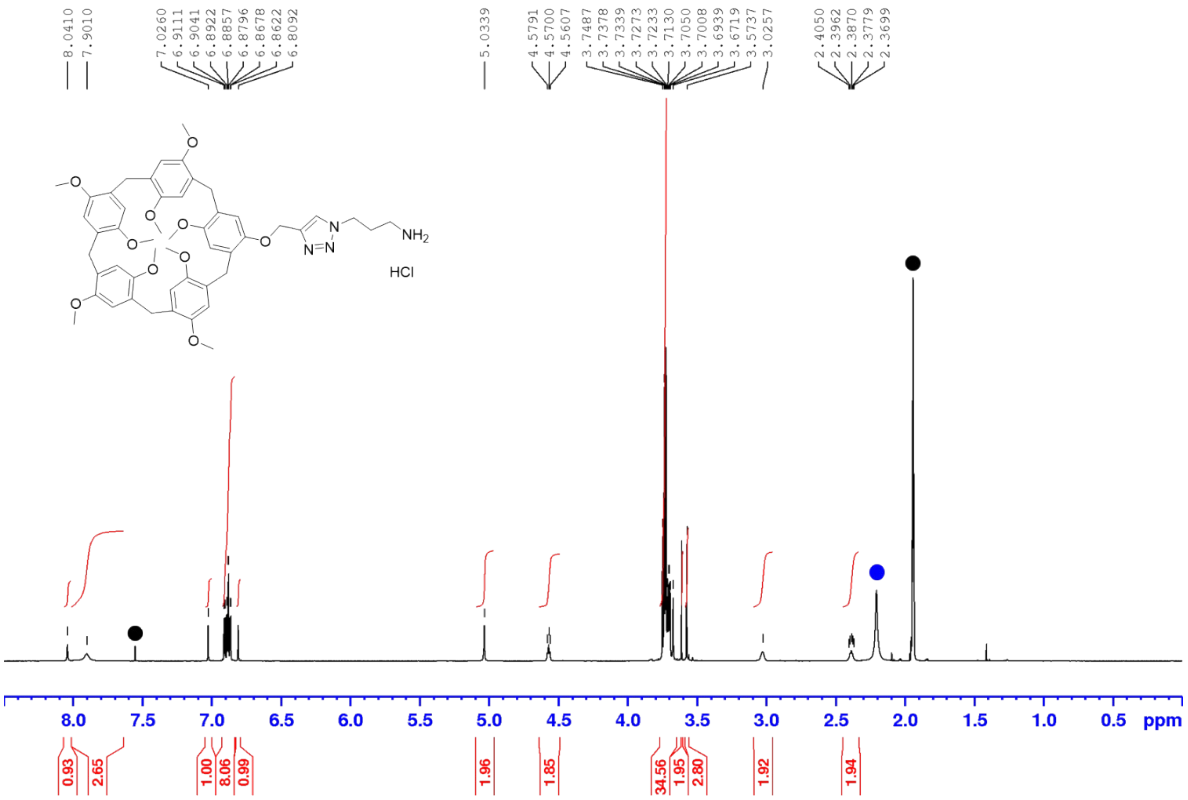

Figure S17. ^{1}H NMR spectrum of HT in $CDCl_3$: CD_3CN (1:3).

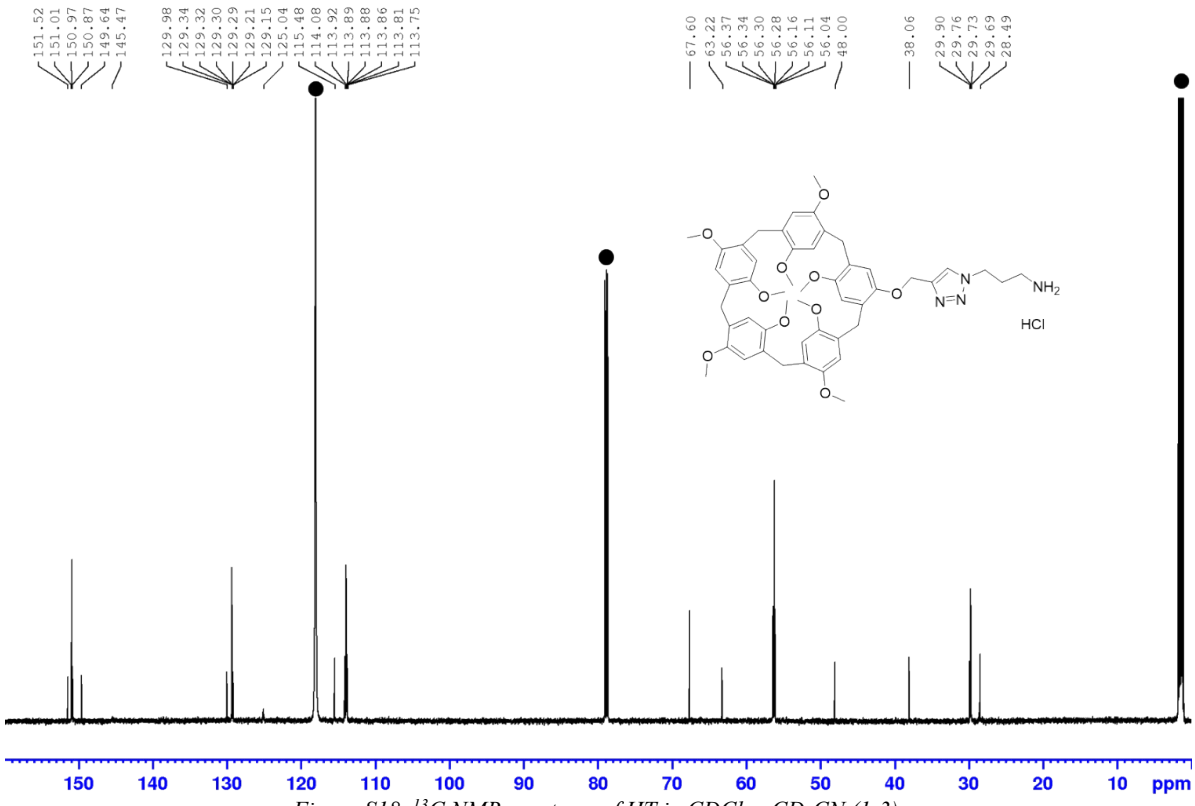

Figure S18. ^{13}C NMR spectrum of HT in $CDCl_3$: CD_3CN (1:3).

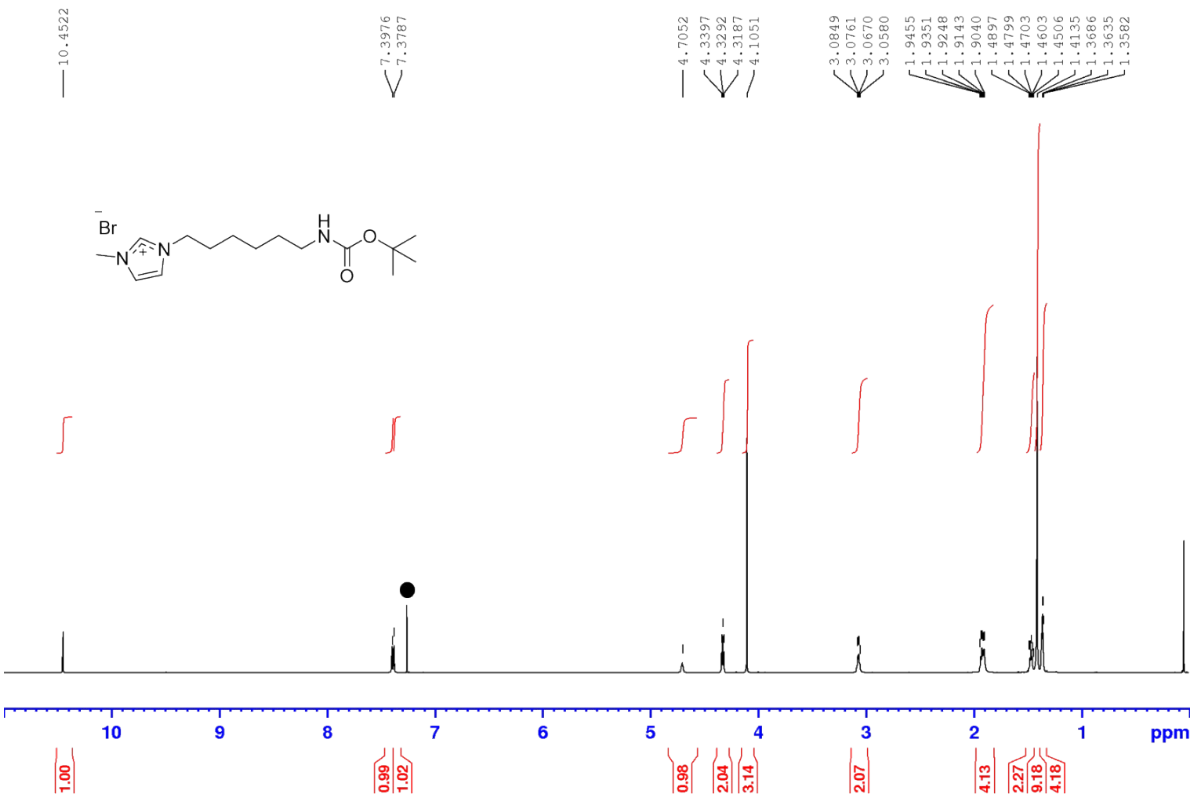

Figure S19. ^{1}H NMR spectrum of MIHA-Boc in $CDCl_3$.

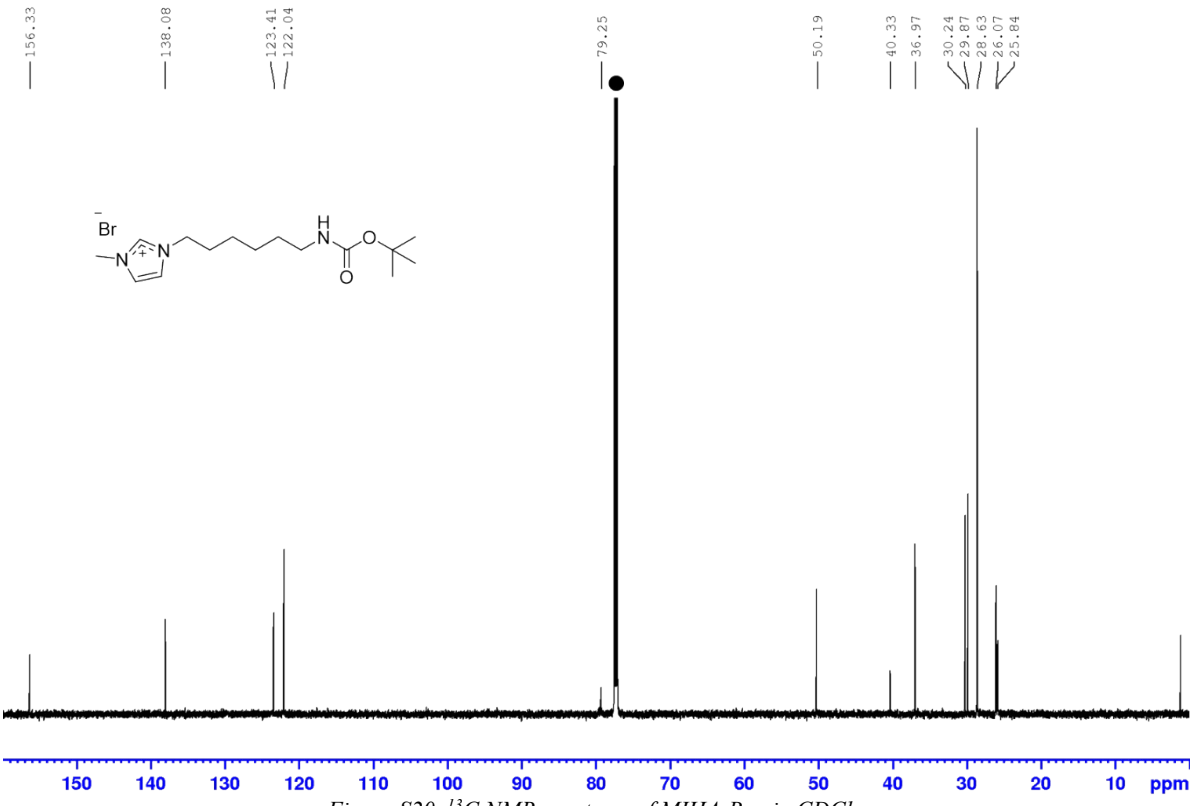

Figure S20. ^{13}C NMR spectrum of MIHA-Boc in $CDCl_3$.

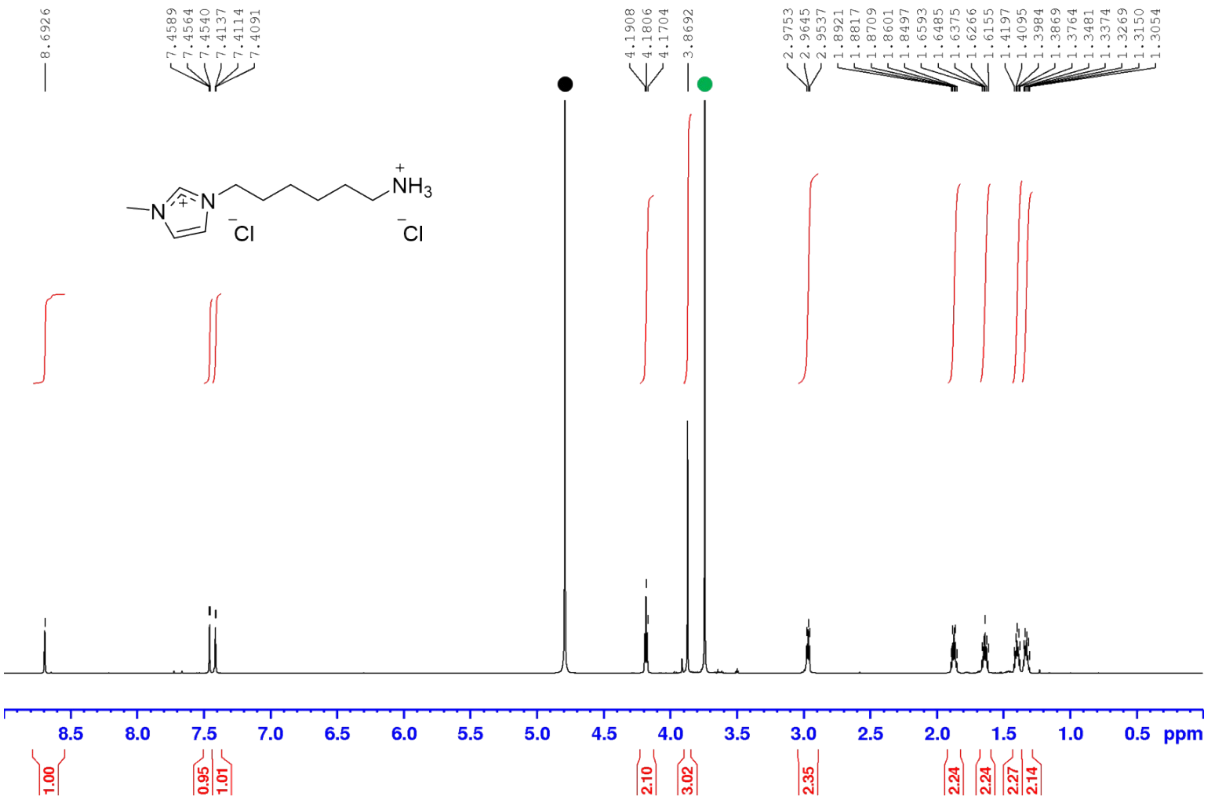

Figure S21. ^{1}H NMR spectrum of MIHA in D_2O.

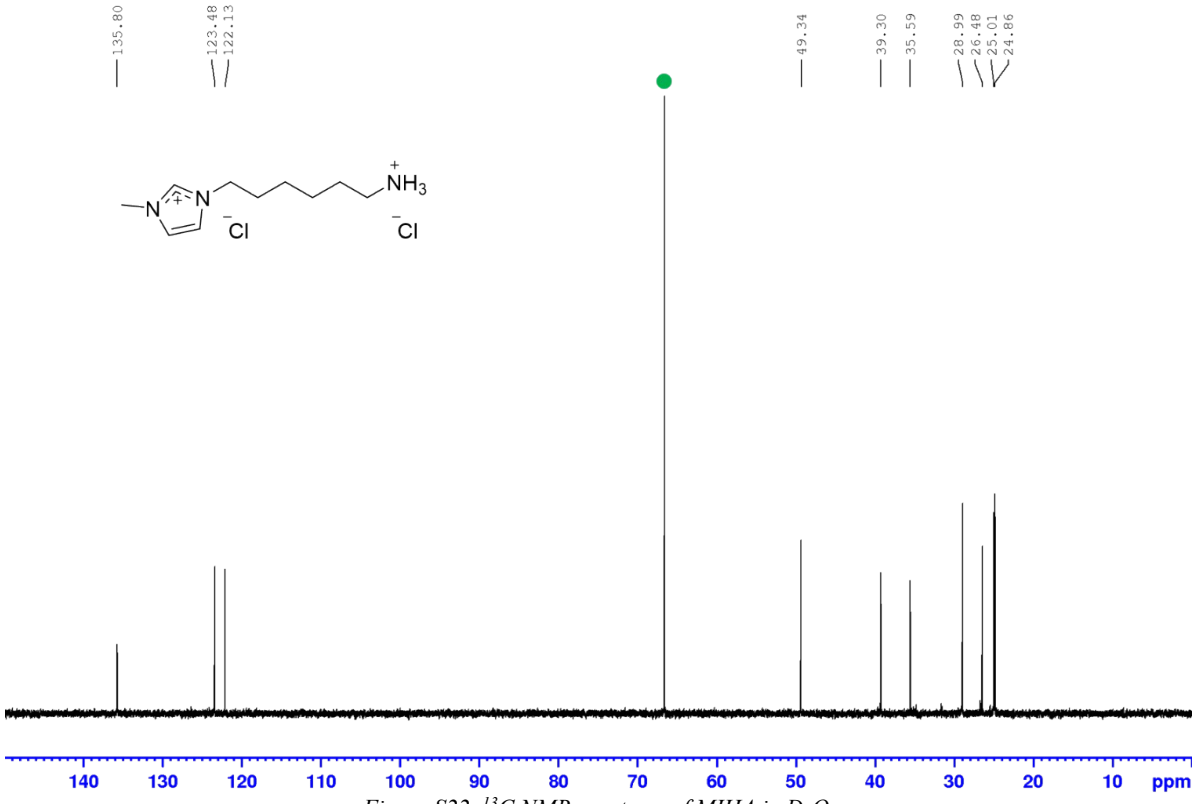

Figure S22. ^{13}C NMR spectrum of MIHA in D_2O.

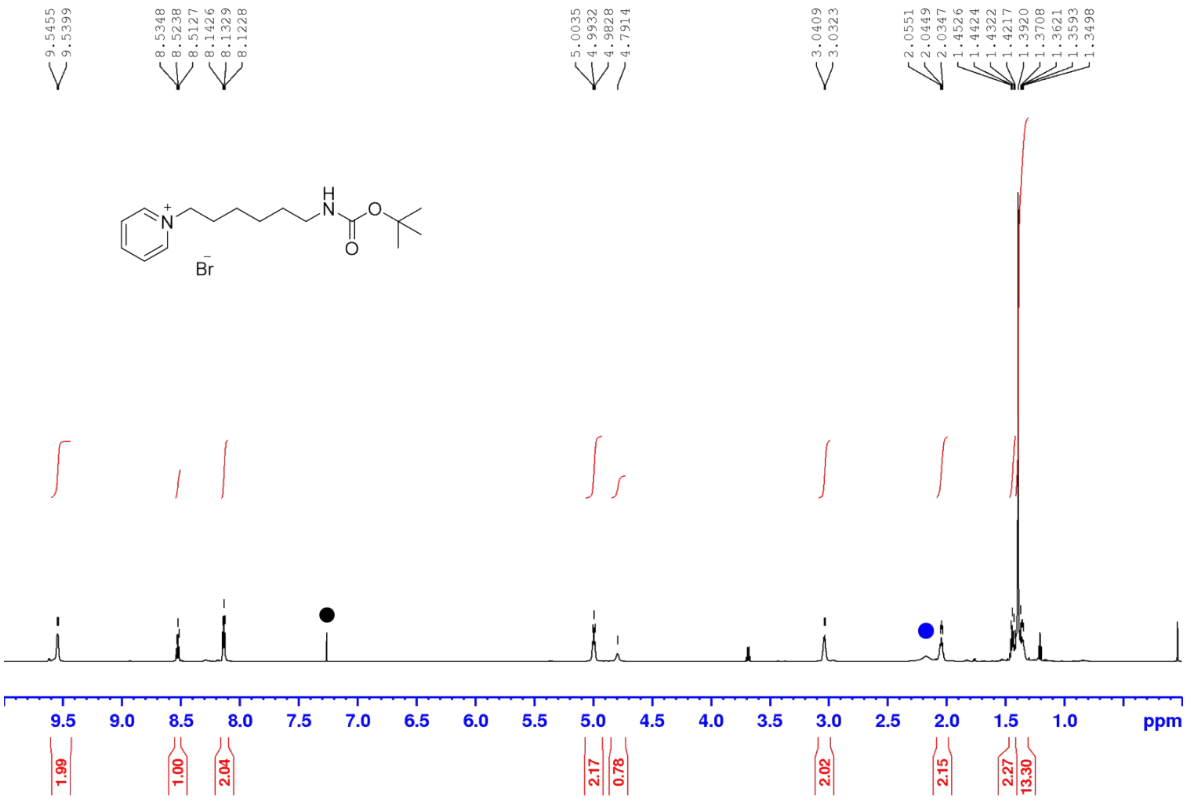

Figure S23. ^{1}H NMR spectrum of PHA-Boc in $CDCl_3$.

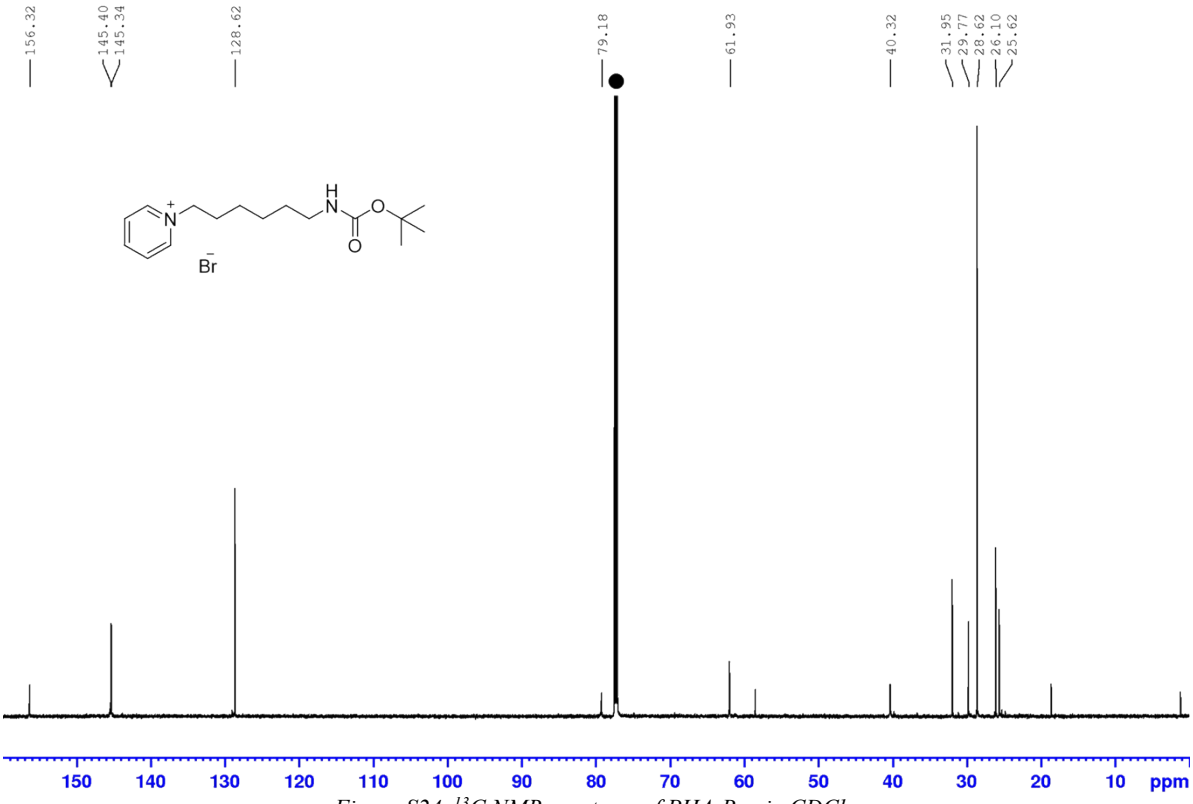

Figure S24. ^{13}C NMR spectrum of PHA-Boc in $CDCl_3$.

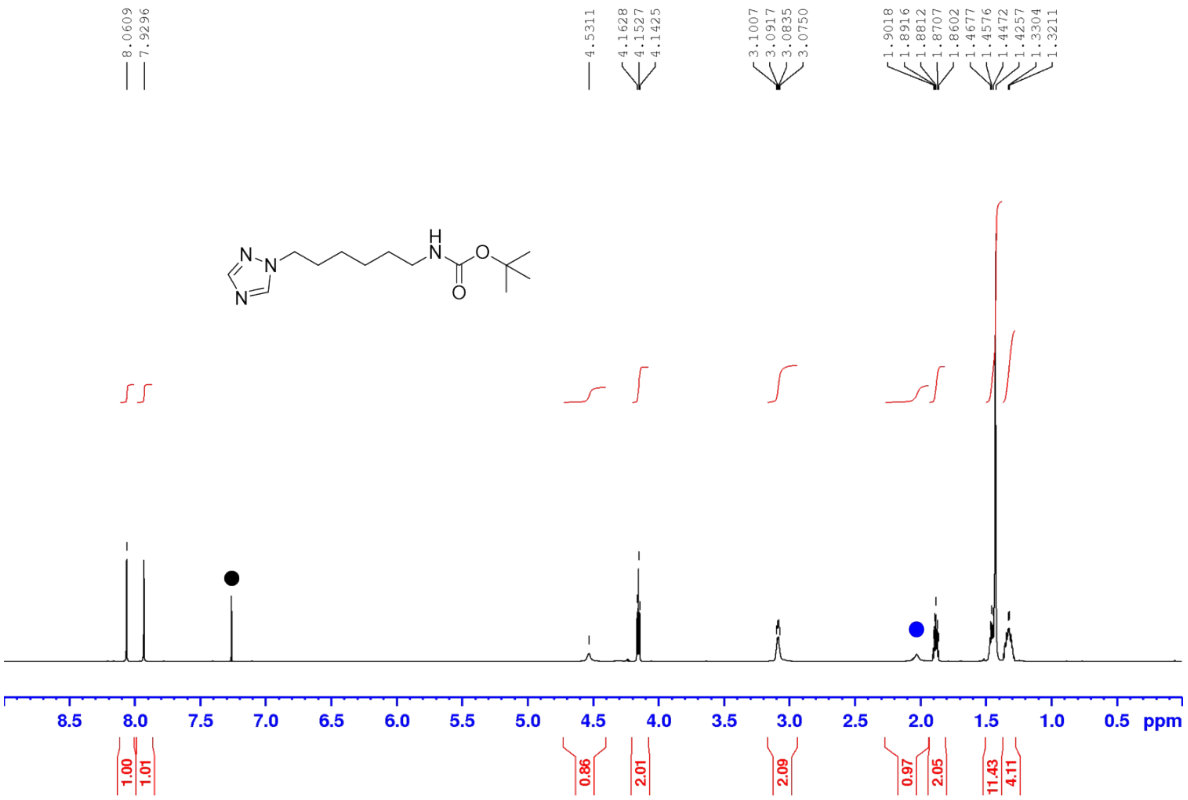

Figure S25. ^{1}H NMR spectrum of THA-Boc in $CDCl_3$.

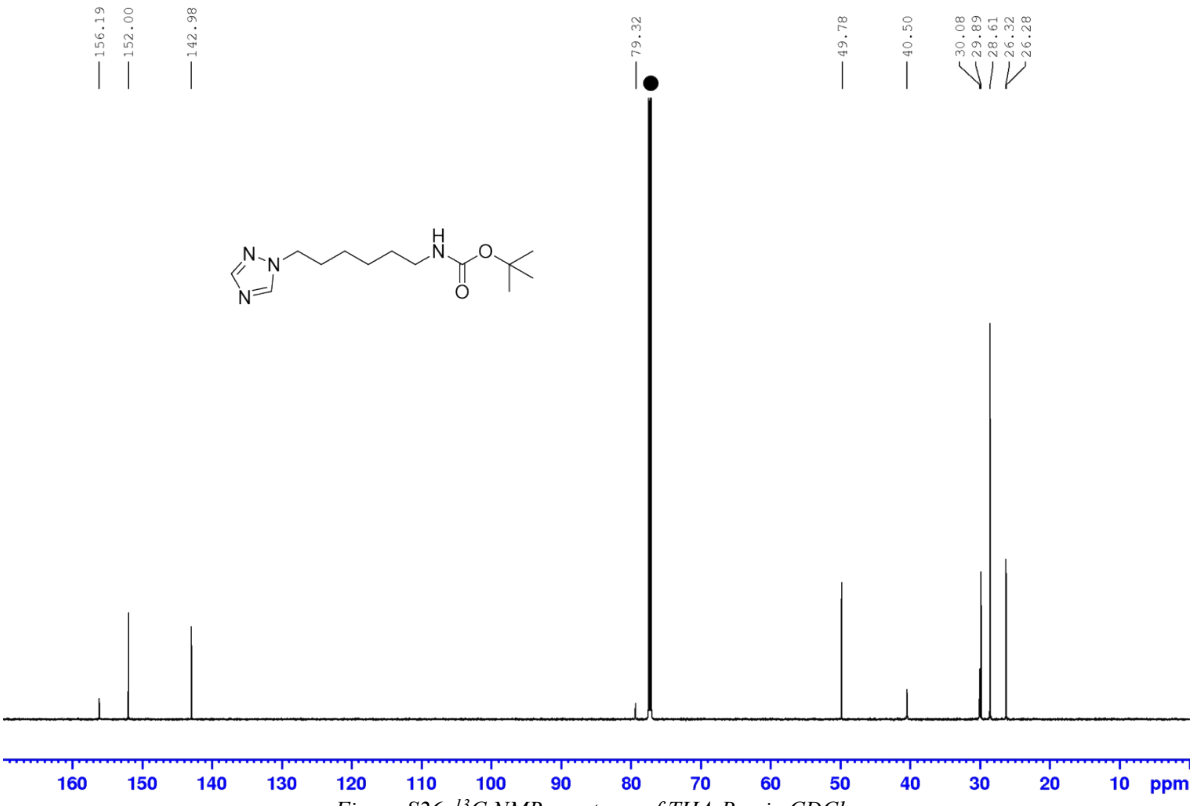

Figure S26. ^{13}C NMR spectrum of THA-Boc in $CDCl_3$.

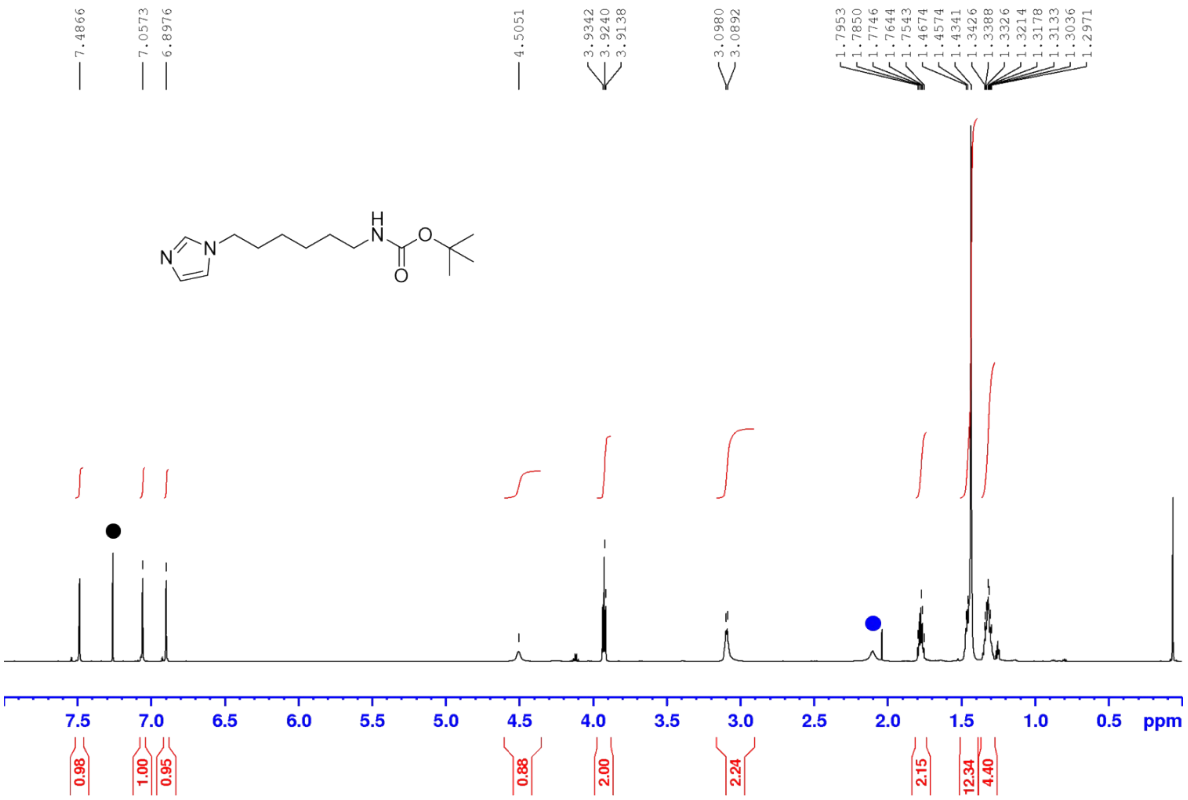

Figure S27. ^{1}H NMR spectrum of IHA-Boc in $CDCl_3$.

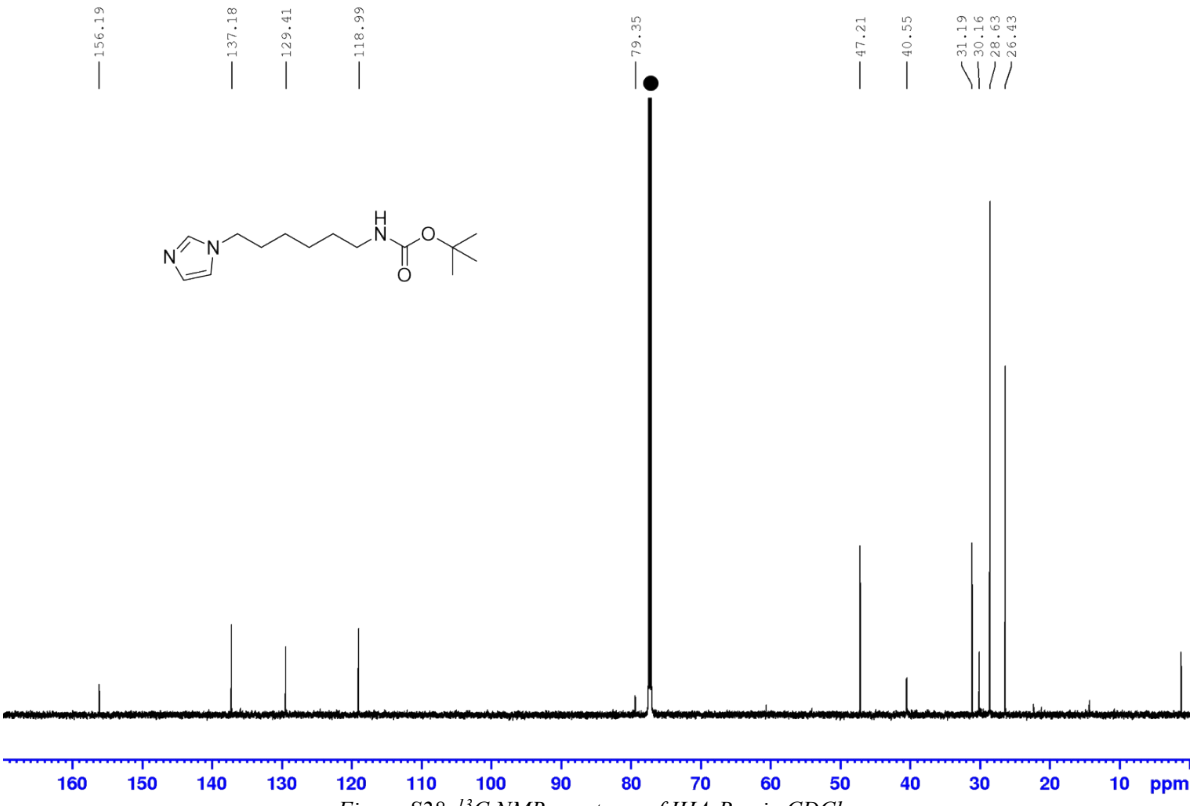

Figure S28. ^{13}C NMR spectrum of IHA-Boc in $CDCl_3$.

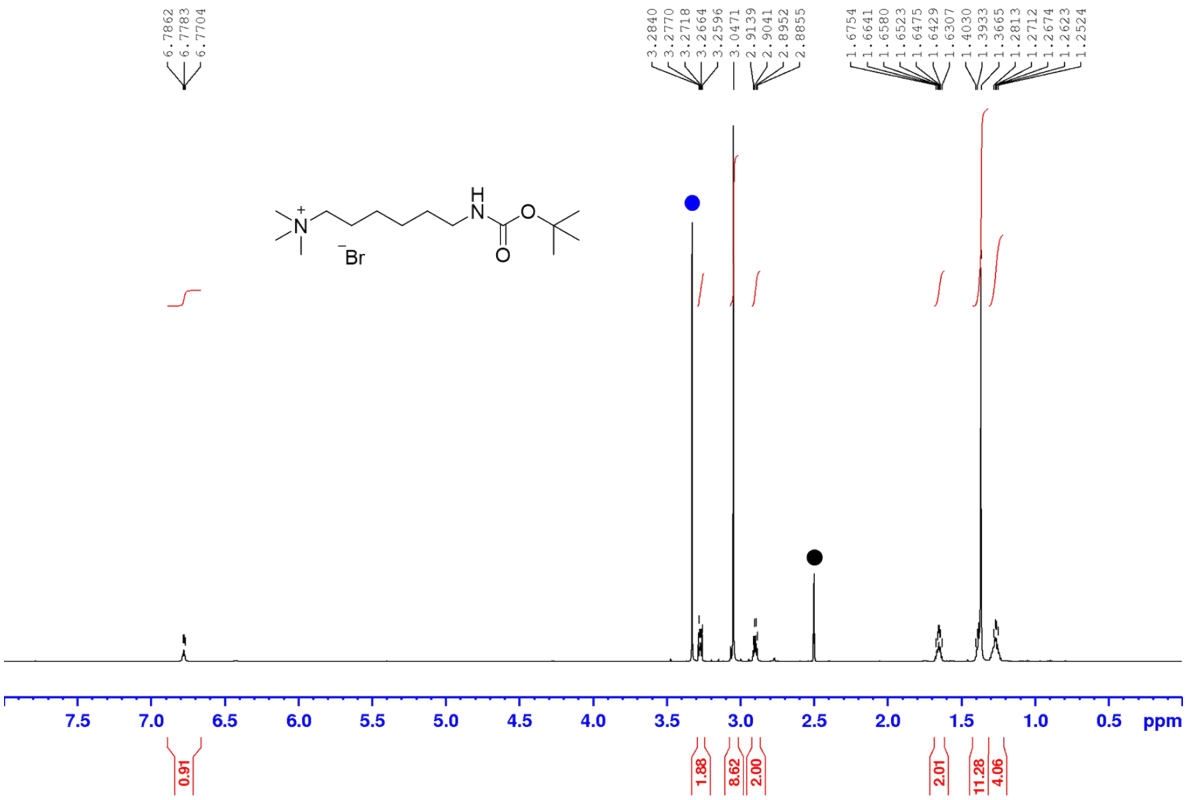

Figure S29. [1]H NMR spectrum of TAHA-Boc in DMSO.

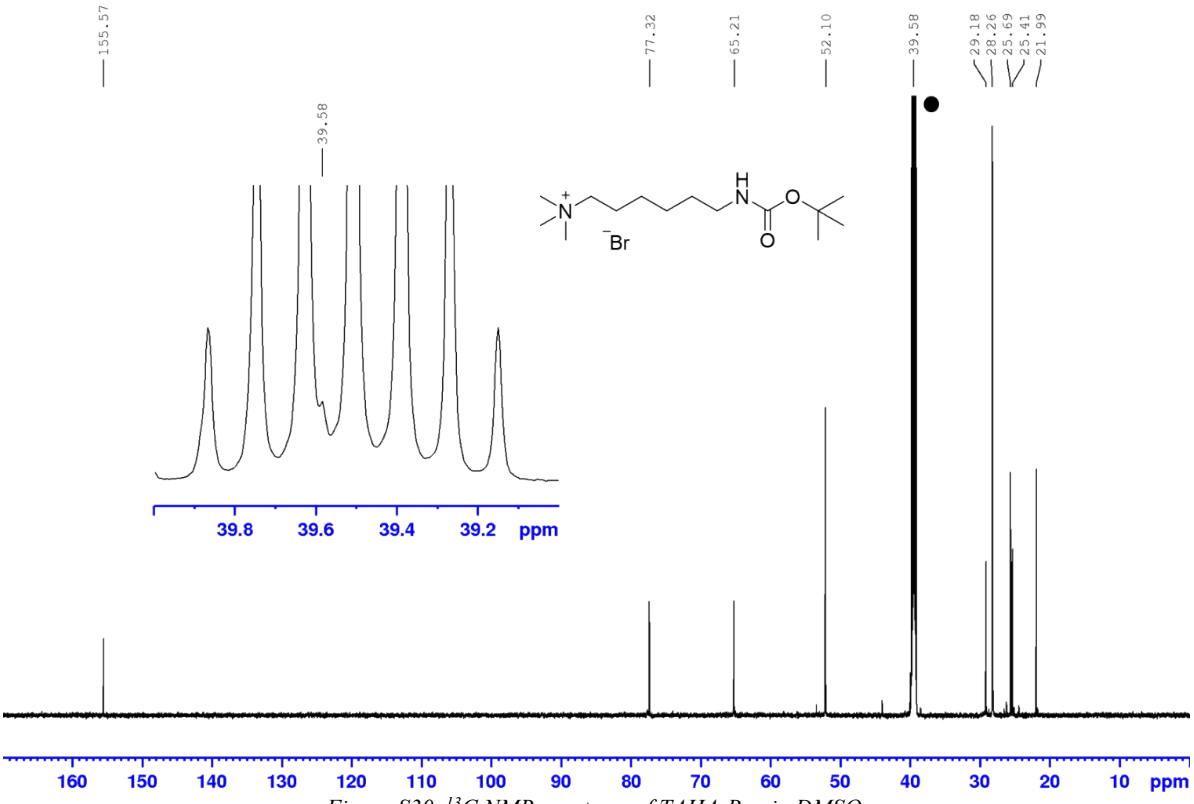

Figure S30. [13]C NMR spectrum of TAHA-Boc in DMSO.

Host-guest complexes investigation

AN@P5A

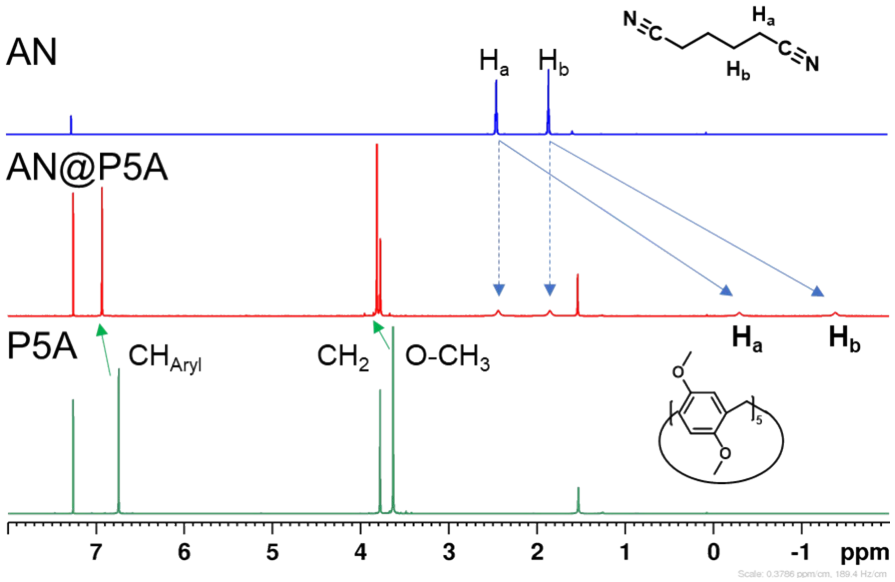

Figure S31. NMR spectra of (from the bottom) P5A, AN@P5A complex (at $[G]_0$: $[H]_0$ = 2.2:1), AN. The change in peak shifts of host and guest is presented by the green and blue arrows, respectively.

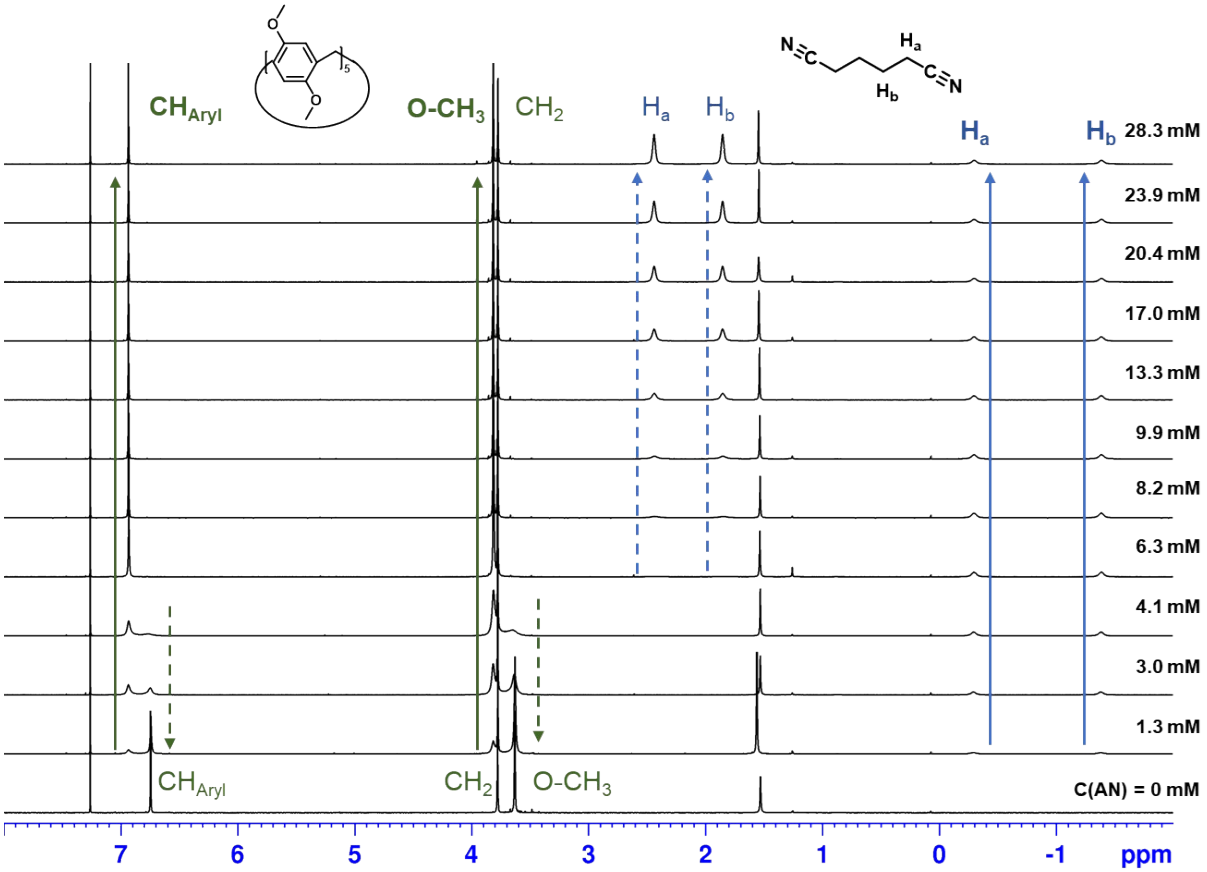

Figure S32. NMR titration of P5A with AN in $CDCl_3$ ($[H]_0$ = 6 mM). Green arrows and letters refer to the P5A, blue ones – to the AN. Solid and dashed lines demonstrate the evolution of the peaks belonging to the complexed and free species, respectively.

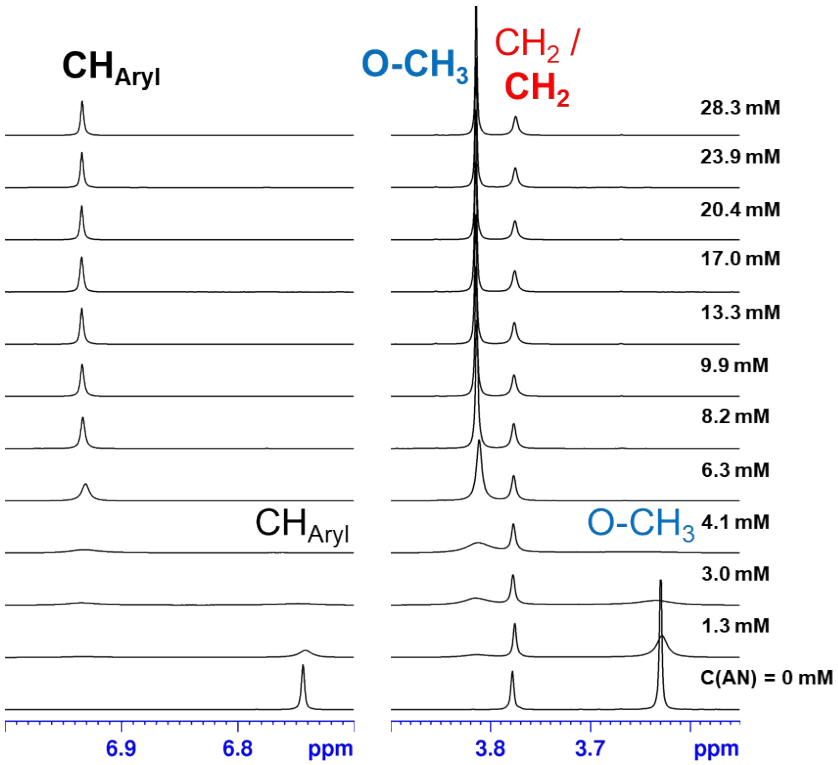

Figure S33. Fragments of the NMR titration (AN@P5A), with only P5A peaks shown. The peaks of the complexed host are depicted in bold.

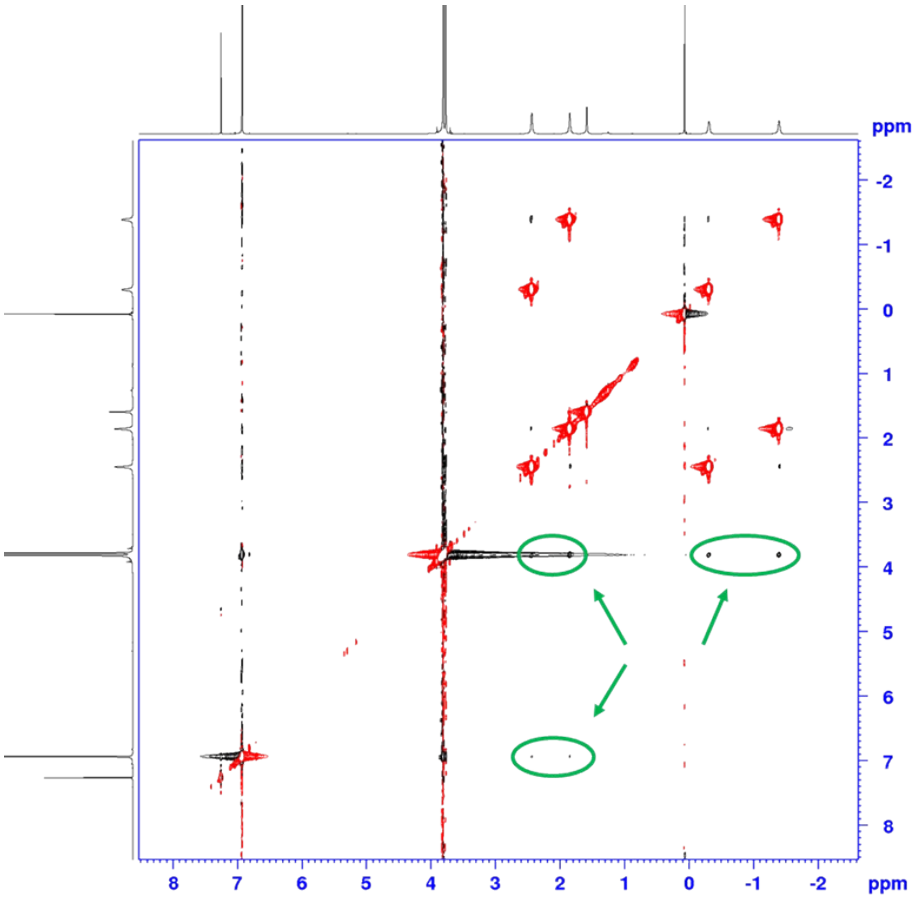

Figure S34. 2D NOESY spectrum of the system P5A–AN (1:2 eq.). NOE cross-peaks indicating proximity between AN and the macrocycle are marked green.

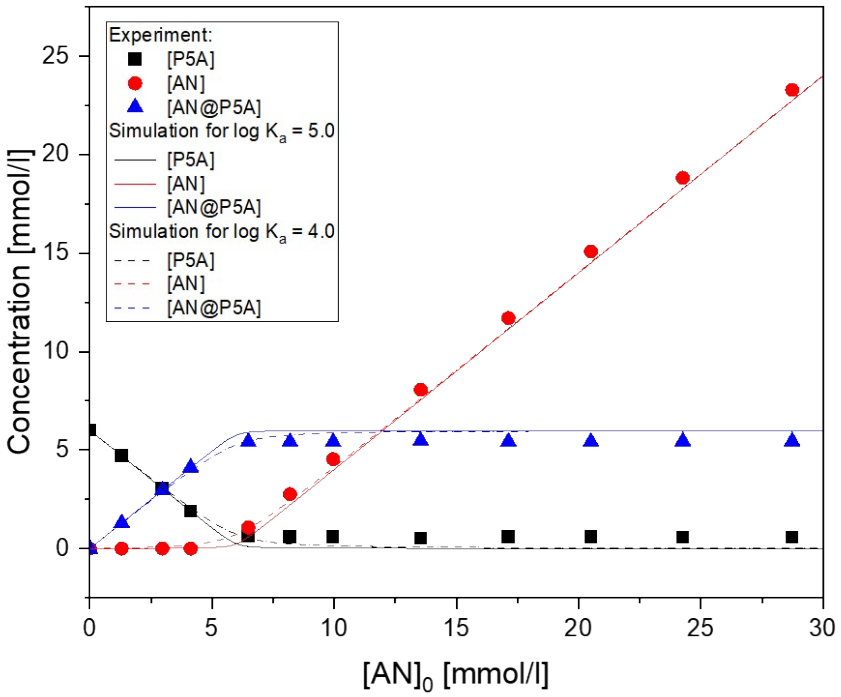

Figure S35. Titration curves for P5A–AN system. Scattered plots: experimental data, line plots: simulated curves for the corresponding species (solid lines: log K_a = 5.0; dashed lines: log K_a = 4.0).

MIHA-Boc@P5A

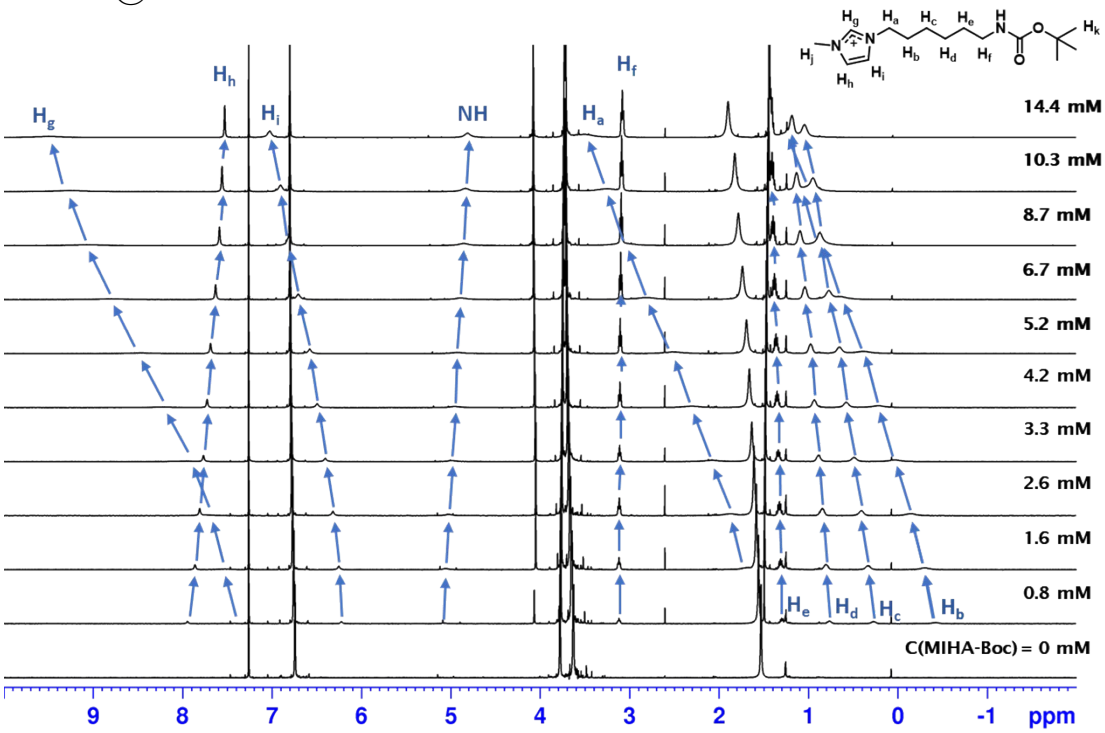

Figure S36. NMR titration of P5A with MIHA-Boc in $CDCl_3$ ($[H]_0$ = 4 mM).

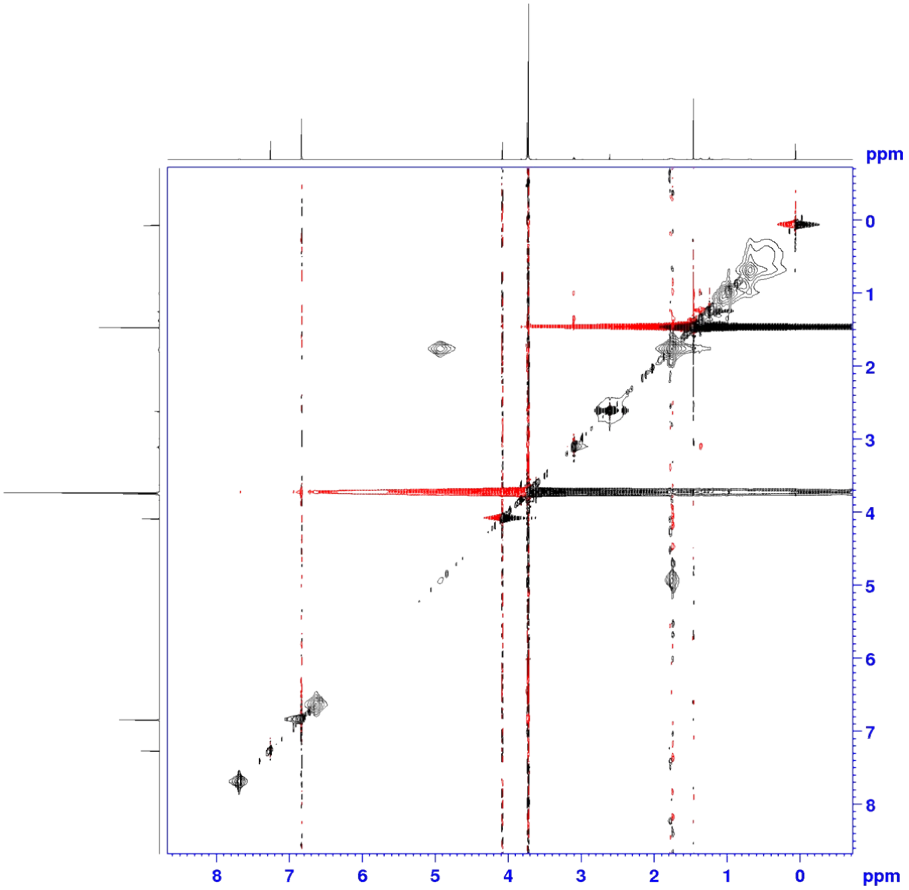

Figure S37. 2D NOESY spectrum of the system P5A–MIHA-Boc (1:1 eq.).

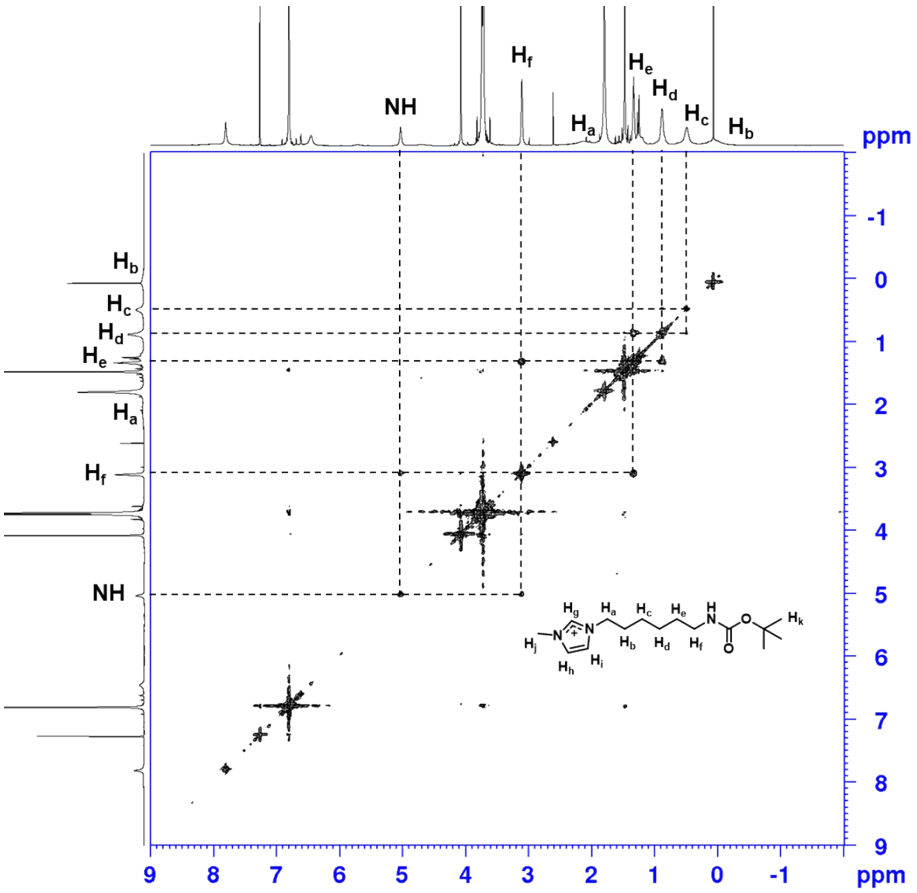

Figure S38. 2D COSY spectrum of the MIHA-Boc@P5A complex.

PHA-Boc@P5A

The NMR titration was conducted in the PHA-Boc concentration range of 0 to 13.0 mM (1:0 to 1:3.25 host:guest ratio, respectively; Figures S39–S41). Similar to the MIHA-Boc@P5A complex, the upfield shift of the alkyl protons H_b–H_e can be traced with decreasing shielding effect strength ($\Delta\delta$ = –2.49 ppm and –0.07 ppm for H_b and H_e, respectively). The shielding effect on the proton H_a is so strong that its signal is not observed in the spectrum of the pseudorotaxane. In contrast to the other proton of the alkyl chain, H_f undergoes a slight deschielding upon P5A presence ($\Delta\delta$ = +0.12 ppm). From the aromatic peaks of the PHA-Boc the significant upfield shift and broadening is exhibited by the *ortho*-proton H_g, suggesting a pronounced shielding due to the inclusion into P5A and coulomb interaction with the electron-rich cavity thereof. Interestingly, even the "outer" *para*-proton H_i exhibits a slight upfield shift whereas the *meta*-proton H_h shifts to the low field. The inclusion complex formation was further supported by 2D NOESY NMR (Figure S43). The spectrum shows cross-peaks corresponding to the interactions between H_h as well as H_d and H_e of PHA-Boc with methoxy groups of P5A.

The maximum of the Job plots (Figure S42, A) indicates a 1:1 stoichiometry of the pseudorotaxane. The binding constant K_a = (4580 ± 980) M^{-1} (log K_a = 3.66 ± 0.09) determined using to the non-linear method (Figure S42, B) is higher than for MIHA-Boc@P5A implying a more stable complex.

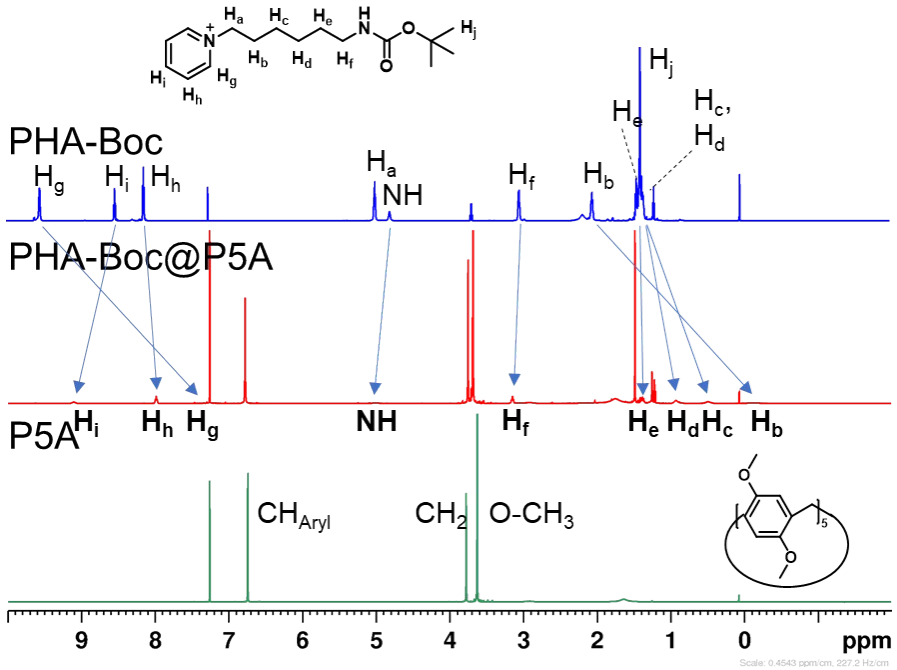

Figure S39. NMR spectra of (from the bottom) P5A, PHA-Boc@P5A complex (at $[G]_0$ = 3.6 mM), PHA-Boc. The change in peak shifts of the guest molecule is presented by the arrows.

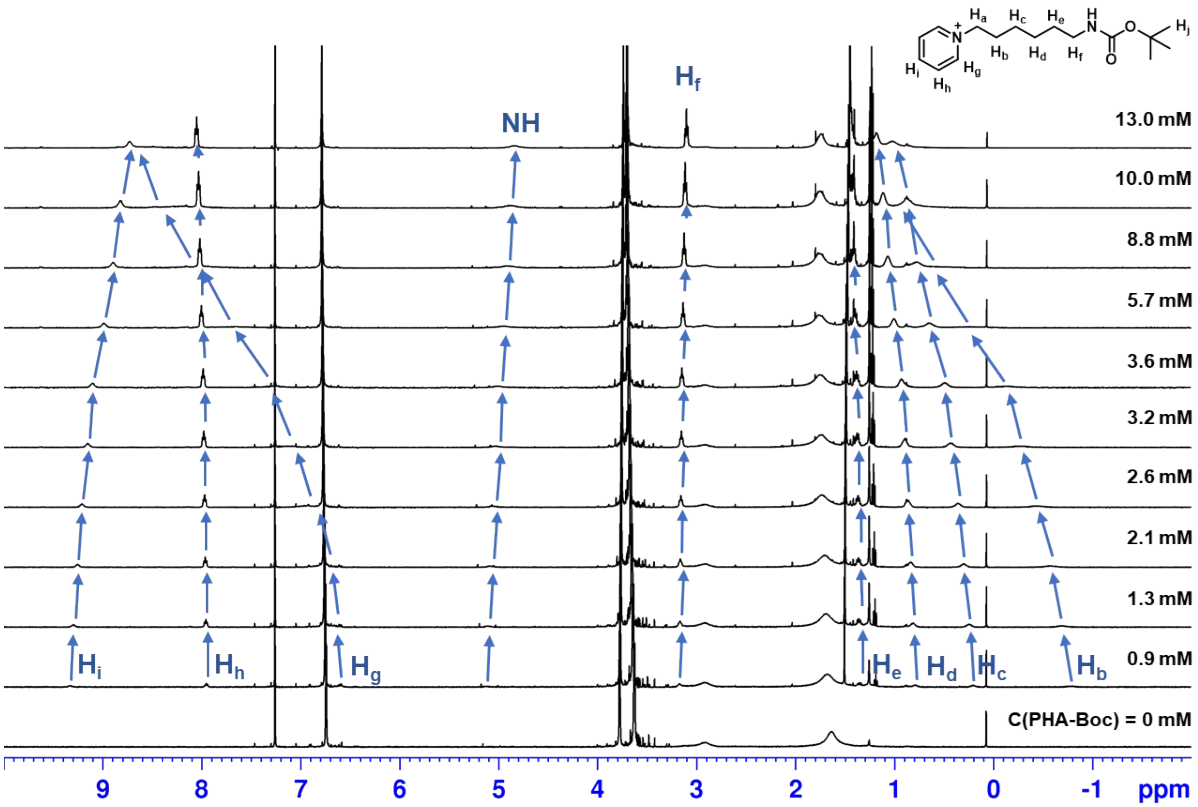

Figure S40. NMR titration of P5A with PHA-Boc in $CDCl_3$ ($[H]_0$ = 4 mM).

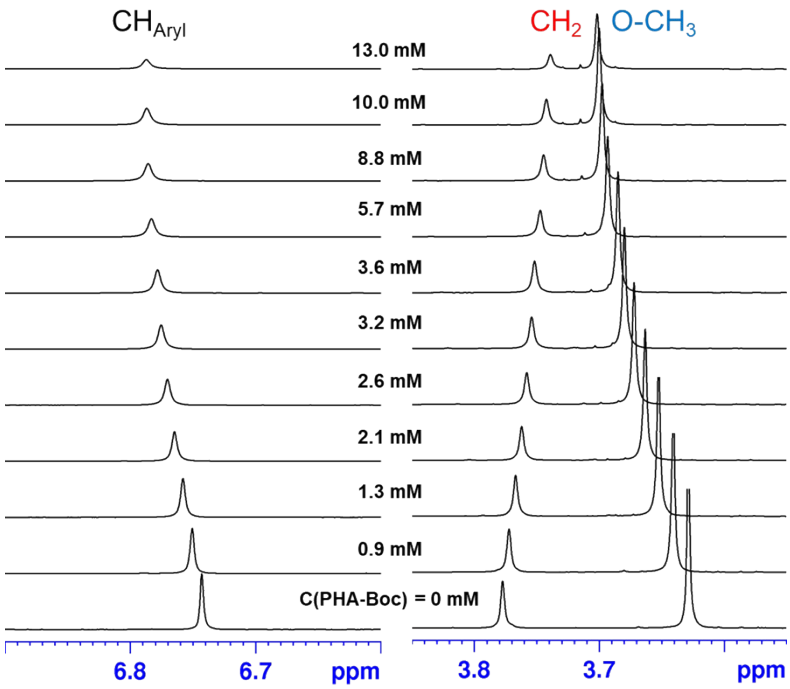

Figure S41. Fragments of the NMR titration (PHA-Boc@P5A), with shifts of only P5A peaks shown.

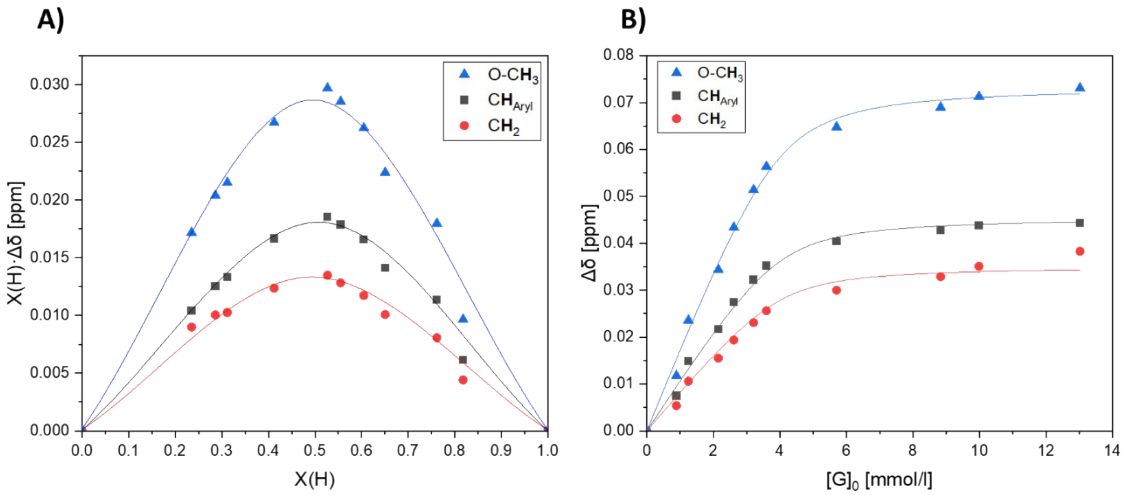

Figure S42. A) Job plot of the P5A–PHA-Boc titration. The maximum of all three peaks of P5A is around 0.5, which proves a 1:1 stoichiometry of the complex (The lines serve as guides for the eye). B) Titration curves corresponding to the P5A protons. The fit curves are obtained using a non-linear least square method with K_a as a common parameter for all dependencies.

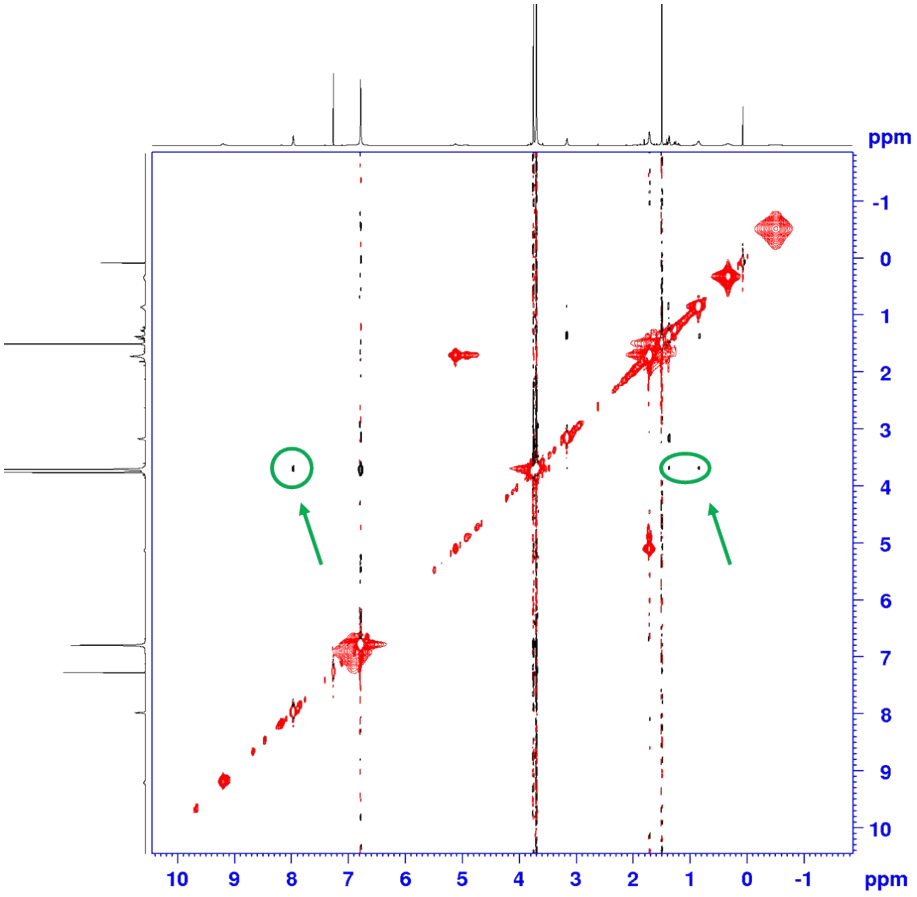

Figure S43. 2D NOESY NMR of the complex PHA-Boc@P5A.
The NOE cross-peaks between host and guest species are marked green.

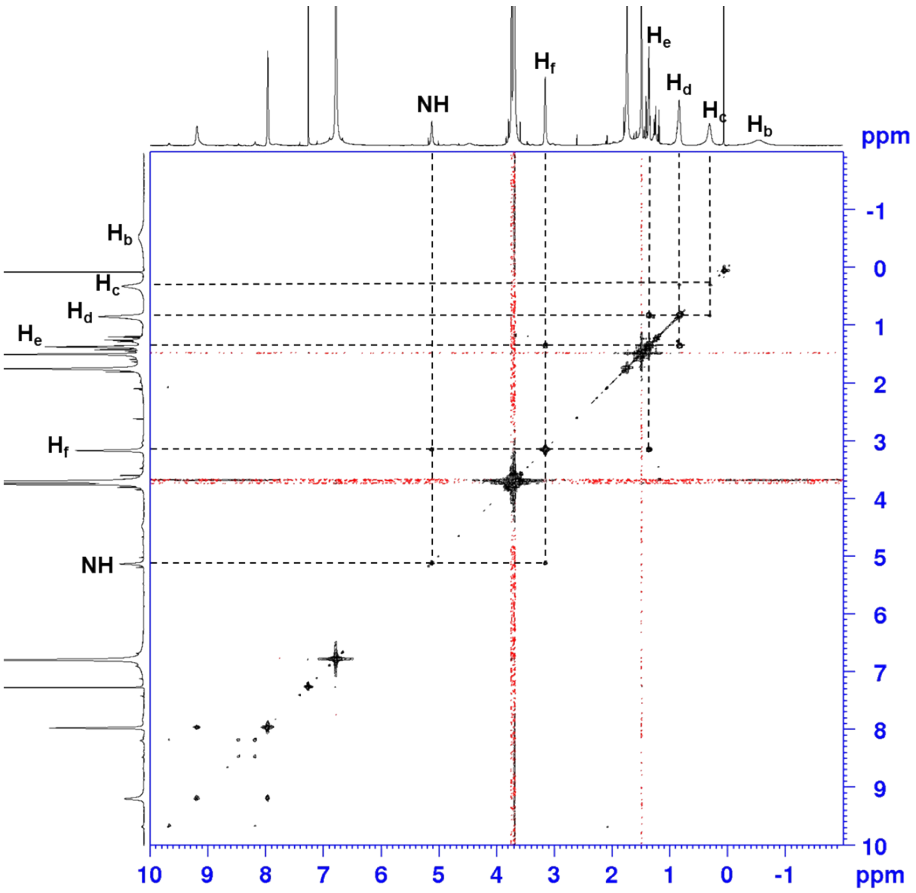

Figure S44. 2D COSY spectrum of the PHA-Boc@P5A complex.

THA-Boc@P5A

The P5A titration with THA-Boc was conducted with the guest concentrations ranging from 0 to 19.2 mM (corresponding to host:guest ratios from 1:0 to 1:3.8; Figure S45–S47). Unlike the previously discussed complexes, the formation of THA-Boc@P5A complex only leads to a broadening of the protons of the guest moiety. Interesting to note the different behavior of the 1,2,4-triazole fragment protons: H_h situated closer to the alkyl chain exhibits strong broadening whereas H_g on the outer side of the heterocycle does not. This might be attributed to the positioning of the guest molecule in the P5A with triazole peeking outside of the cavity. Due to such placement the outer proton H_g is not screened by the macrocycle and, therefore, its relaxation proceeds slower compared to the proton H_g, which results in a sharp peak even in a complexed state.

The host-guest complex formation was further proven by NOESY NMR (Figure S49). The cross-peaks between triazole protons and the methyl as well as aromatic protons of P5A (highlighted green), demonstrate that the triazole tail of the THA-Boc are in proximity to the protons of the cavity. However, since H_g and H_f overlap in the investigated ^{1}H NMR spectra, it is not possible to determine which of the protons interacts with P5A.

The stoichiometry of the pseudorotaxane is determined with the Job plot (Figure 48, A) to be 1:1, which allows the application of the 1:1 binding model to calculate the complexation constant: $K_a = 185 \pm 18\ M^{-1}$ ($\log K_a = 2.27 \pm 0.04$) (Figure 48, B).

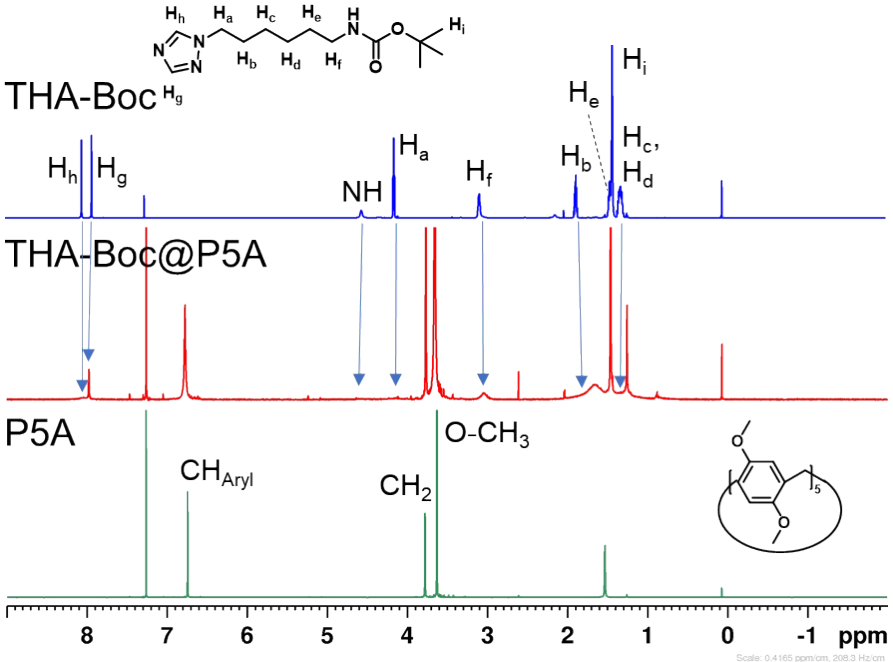

Figure S45. NMR spectra of (from the bottom) P5A, THA-Boc@P5A complex (at $[G]_0 = 4.0$ mM), THA-Boc.

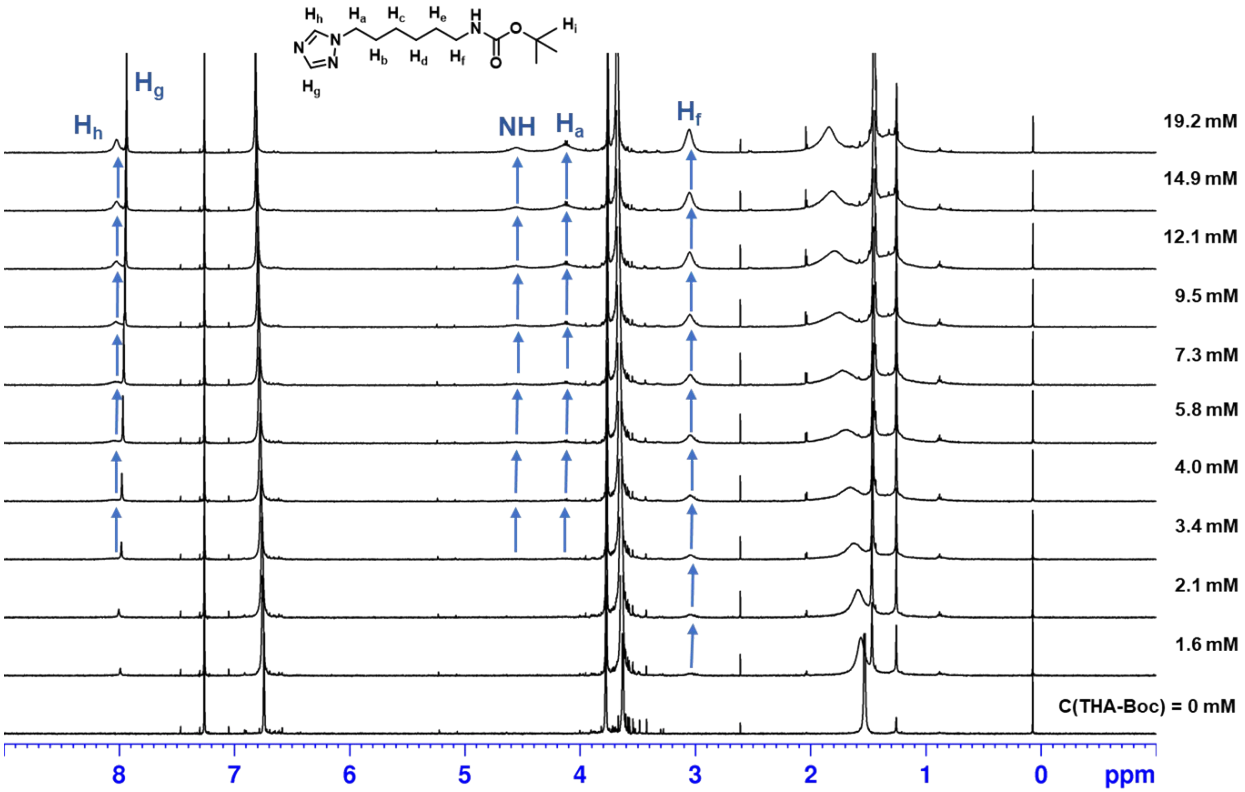

Figure S46. NMR titration of P5A with THA-Boc in $CDCl_3$ ($[H]_0$ = 4 mM).

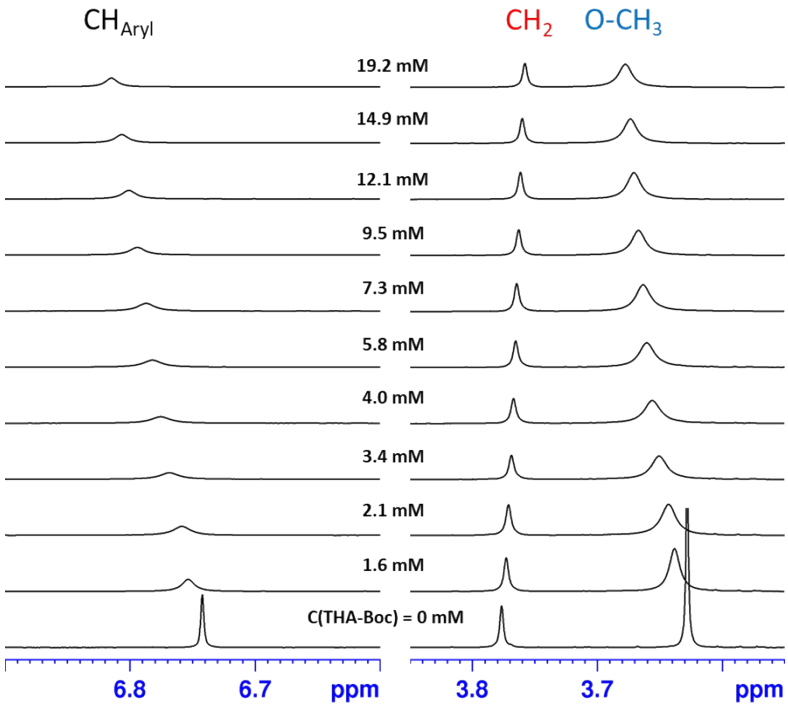

Figure S47. Fragments of the NMR titration (THA-Boc@P5A), with shifts of only P5A peaks shown.

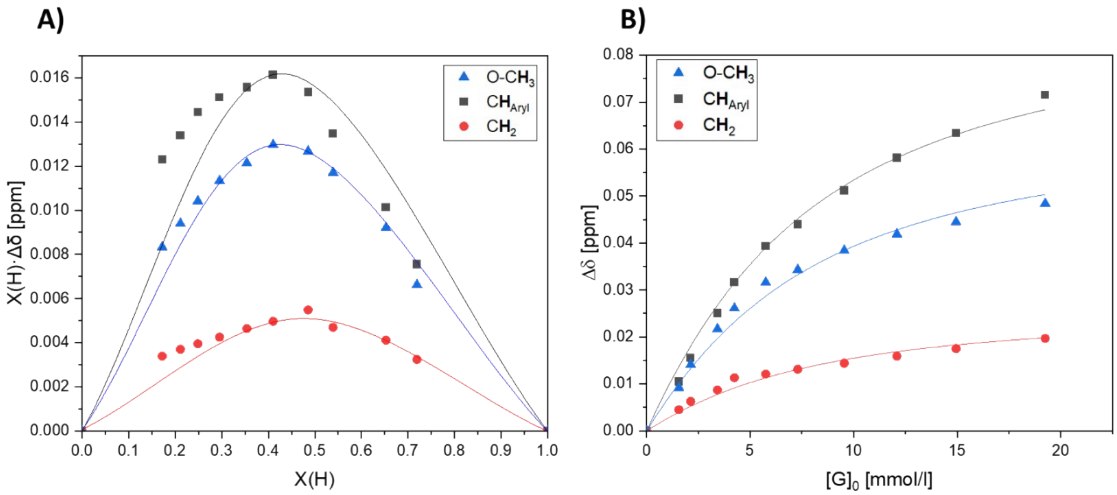

Figure S48. A) Job plot of the P5A–THA-Boc titration. The maximum of all three peaks of P5A is around 0.5, which proves a 1:1 stoichiometry of the complex (The lines serve as guides for the eye). B) Titration curves corresponding to the P5A protons. The fit curves are obtained using a non-linear least square method with K_a as a common parameter for all dependencies.

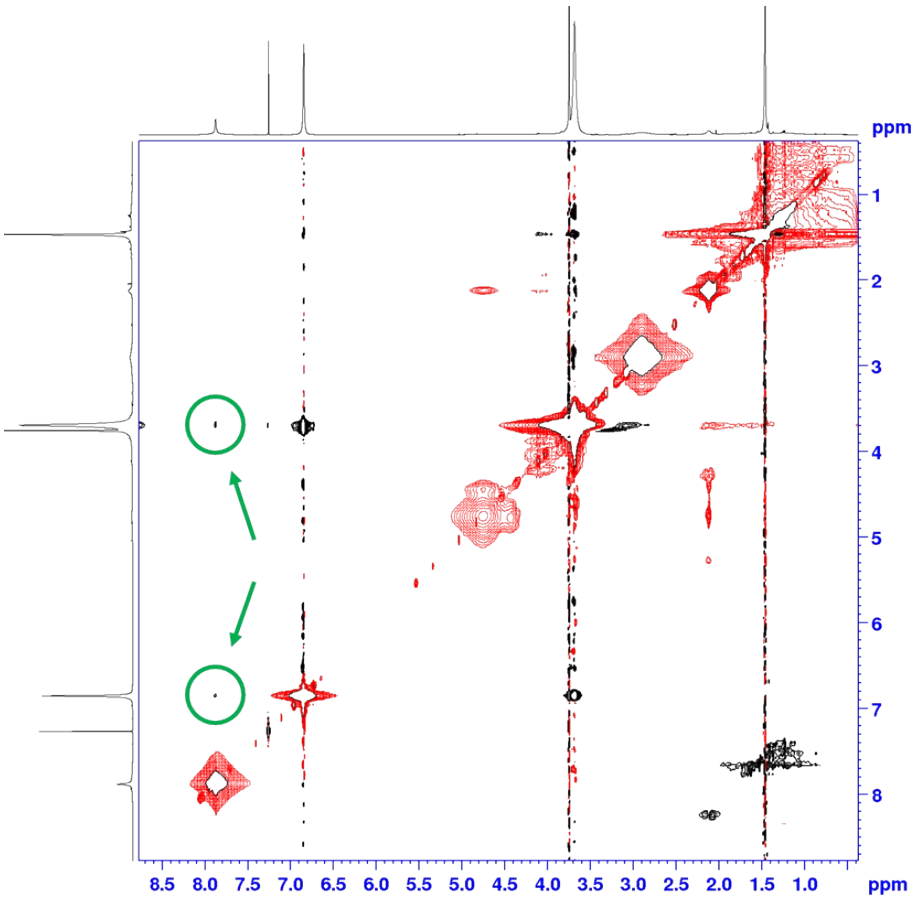

Figure S49. 2D NOESY NMR of the complex THA-Boc@P5A.
The NOE cross-peaks between host and guest species are marked green.

Table S1. Binding constants and chemical shift at full complexation determined by NMR-titration

Complex	Log K_a	$O\text{-}CH_3$		CH_{Aryl}		CH_2	
		$\Delta\delta_{max}$, ppm	R^2	$\Delta\delta_{max}$, ppm	R^2	$\Delta\delta_{max}$, ppm	R^2
MIHA-Boc@P5A	3.32 ± 0.10	0.092 ± 0.002	0.9853	0.064 ± 0.002	0.9926	0.042 ± 0.002	0.9680
PHA-Boc@P5A	3.66 ± 0.09	0.074 ± 0.001	0.9950	0.046 ± 0.001	0.9947	0.035 ± 0.001	0.9813
THA-Boc@P5A	2.27 ± 0.04	0.066 ± 0.003	0.9853	0.090 ± 0.003	0.9926	0.026 ± 0.001	0.9680

IHA-Boc@P5A

The system IHA-Boc@P5A is a slow-exchange complex as indicated by the presence of both free and bound species on the spectra (Figures S50–S52). As is the case with other host-guest complexes in this work, the methylene protons of the hexane chain undergo a strong shielding with a difference in chemical shift for the proton H_a reaching $\Delta\delta = -3.43$ ppm. The stoichiometry is determined by the integration of the peaks corresponding to the complexed P5A and IHA-Boc which interestingly revealed a 1:2 (P5A:IHA-Boc) geometry for the whole range of titration ratios. Although the spectra contain only one set of peaks belonging to complexed species, the peaks of alkyl protons of IHA-Boc shielded by the complexation noticeably shift upon increasing IHA-Boc concentration (Figure S51). Surprisingly, unlike aforementioned MIHA-Boc@P5A or PHA-Boc@P5A whose alkyl peaks exhibit deshielding upon guest addition due to an increasing uncomplexed species ratio, the peaks of IHA-Boc (H_c and H_d) shift upfield suggesting an enhanced shielding and, therefore, a higher ratio of guest molecules taking part in the pseudorotaxane formation. This implies a three-state equilibrium between free host, free guest and two complex species in the solution:

$$H + 2G \overset{K_1}{\leftrightarrow} HG + G \overset{K_2}{\leftrightarrow} HG_2$$

From these processes taking place in the system the first equilibrium (K_1) is plausibly slow on NMR timescale, whereas the second one (K_2) is fast, hence, the positions of peaks of H_c and H_d resemble the weighted average between two- and three-component complexes. The in-depth determination of the parameters underlying the interaction between IHA-Boc and P5A requires further investigations which are out of the scope of the present study.

The complexation constant K_a was calculated using the following equation from the spectrum of 1:2 (host:guest) mixture:

$$K_a = K_1 \cdot K_2 = \frac{[HG_2]}{[H][G]^2} = 7900\ M^{-2}$$

where $[HG_2]$ is the concentration of the complex $(IHA\text{-}Boc)_2$@P5A, [H] and [G] are the concentrations of free P5A and IHA-Boc, respectively.

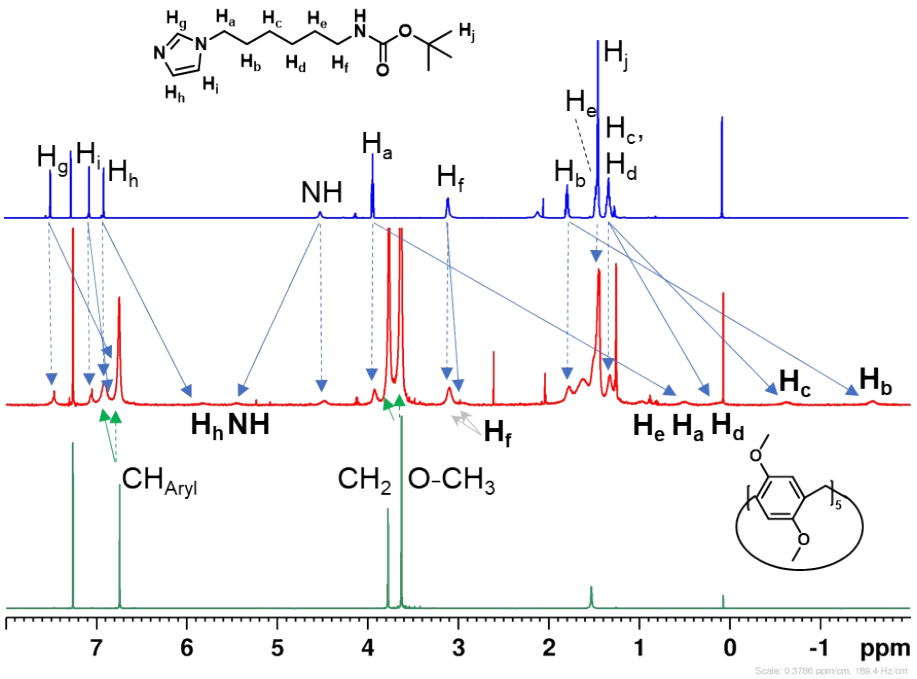

Figure S50. NMR spectra of (from the bottom) P5A, IHA-Boc@P5A complex (at $[G]_0$ = 4.9 mM), IHA-Boc. The change in peak shifts of the molecules is presented by solid arrows; dashed arrows demonstrate the peaks of the free species.

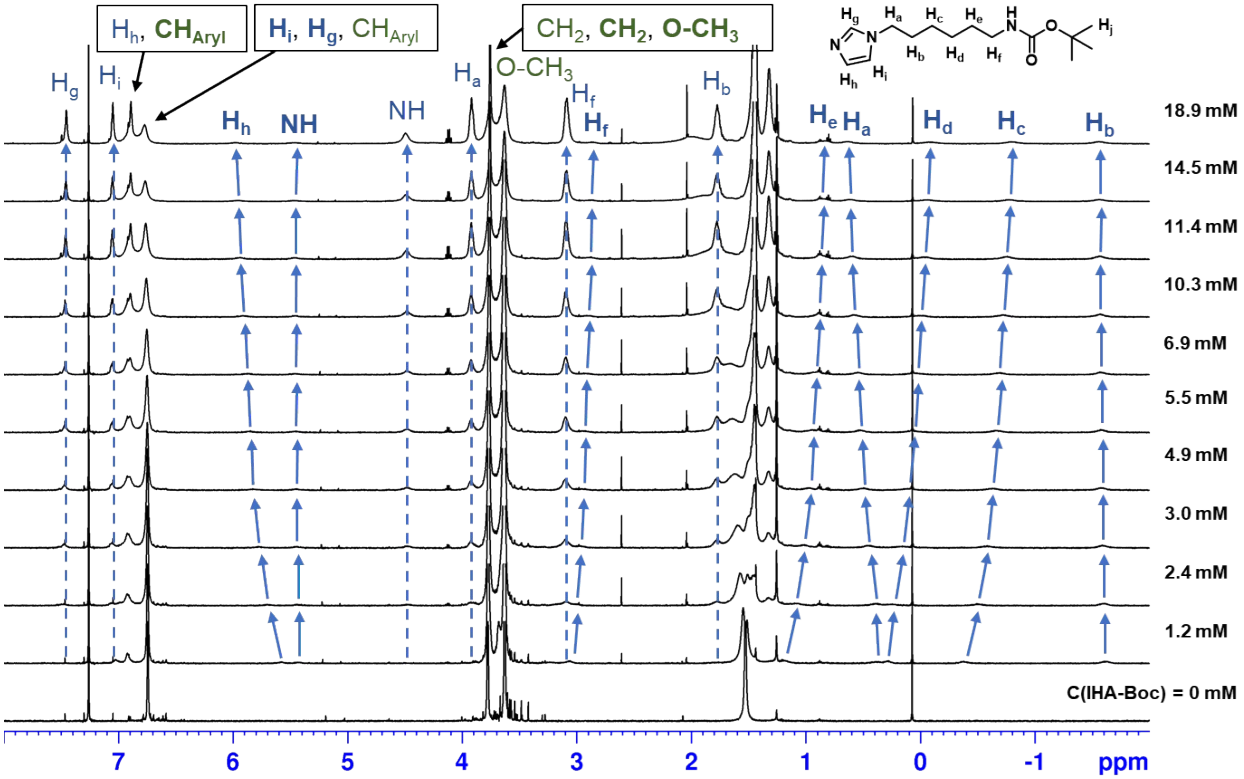

Figure S51. NMR titration of P5A with IHA-Boc in $CDCl_3$ ($[H]_0$ = 4 mM). Normal and bold designations refer to free and complexed species.

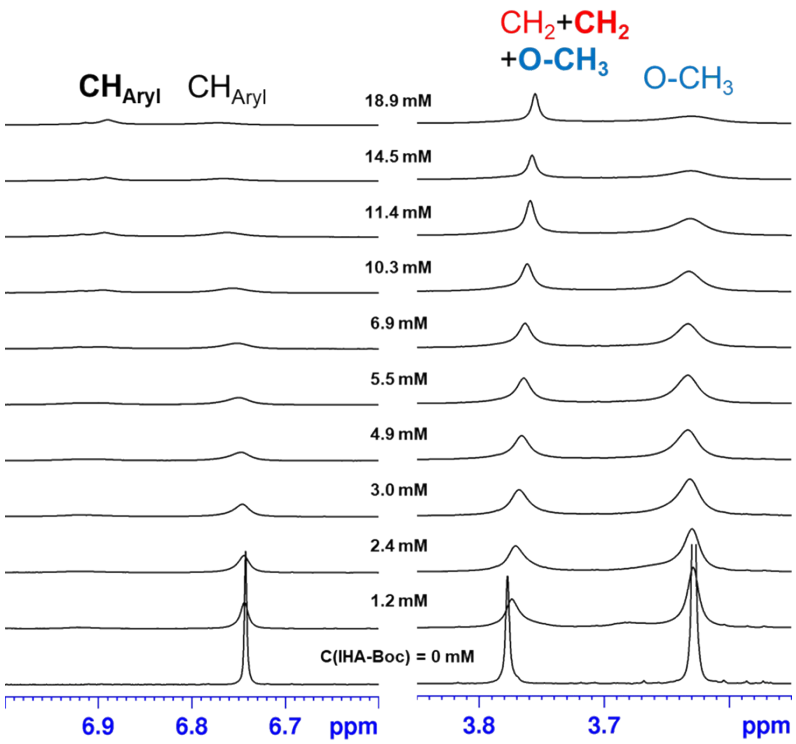

Figure S52. Fragments of the NMR titration (IHA-Boc@P5A), with shifts of only P5A peaks shown.

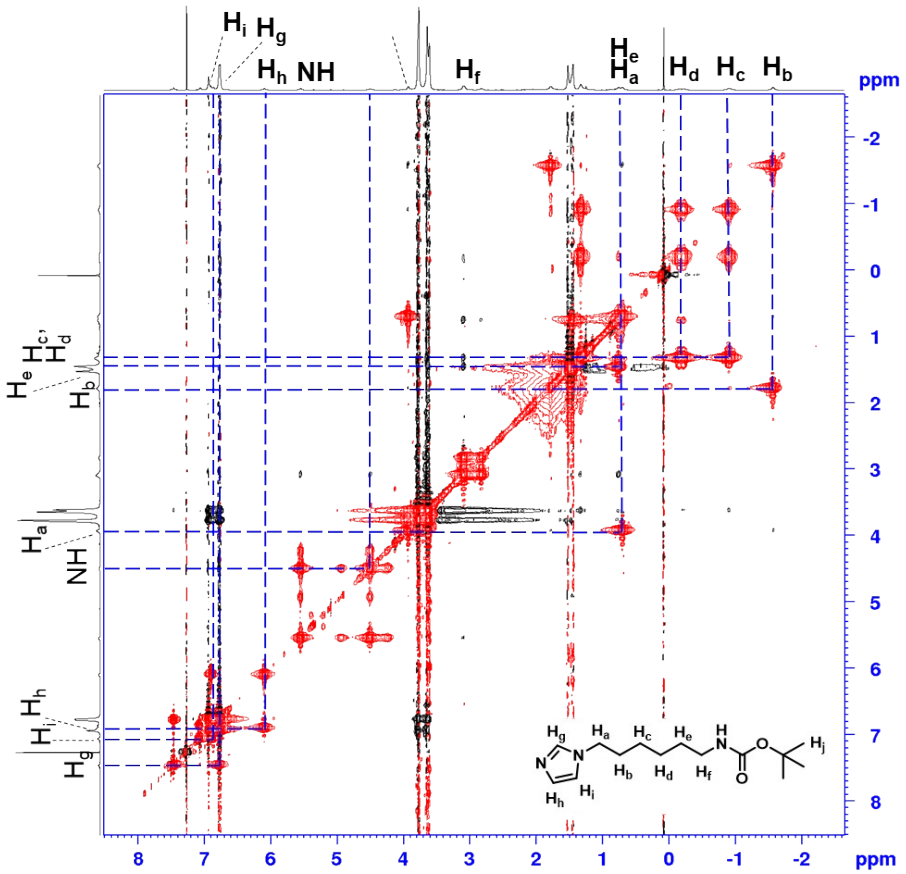

Figure S53. 2D NOESY NMR of the complex IHA-Boc@P5A. The blue dashed lines represent the relation between the peaks of the free and bound guest. On the horizontal and vertical projections, the peaks of a bound and free (respectively) guest are marked.

TAHA-Boc@P5A

In the case of TAHA-Boc the interaction between host and guest is also slow on the NMR timescale (Figure S54–S56). Alkyl peaks belonging to the axle included into the P5A cavity are strongly shifted upfield compared to the free TAHA-Boc, and similar to the other complexes the upfield shift and, hence, shielding of the protons decreases from H_a to H_e ($\Delta\delta$ = –3.15 ppm and +0.01 ppm, respectively). The protons of the methyl groups of the quaternary ammonium tail exhibit likewise a shift to the high field as well as a significant broadening. These protons are further shown by the NOE cross-peak on the 2D NOESY spectrum to be in a proximity of P5A methoxy groups (Figure S58). These findings suggest the placement of the guest moiety with its ammonium tail inside of P5A. The stoichiometry of the pseudorotaxane was determined by the peak integration to be 1:1 (host:guest), and the binding constant was calculated from the 1:1 mixture to be log K_a = 2.53 ± 0.03.

The titration curves simulated for a system with log K_a = 2.53 align well with the experimental data for the beginning of the titration, as shown on the Figure S57.

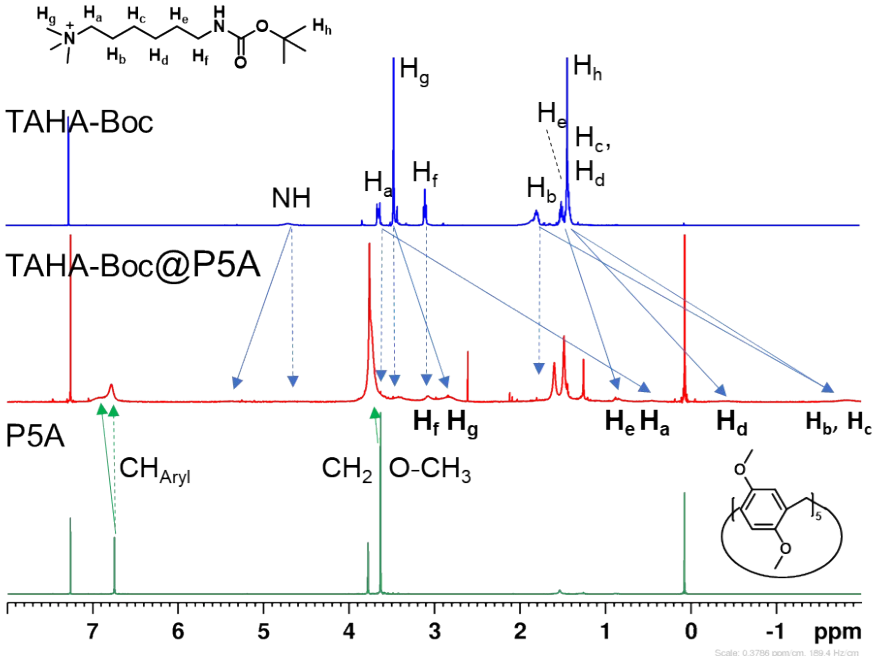

Figure S54. NMR spectra of (from the bottom) P5A, TAHA-Boc@P5A complex (at $[G]_0$ = 4.3 mM), TAHA-Boc. The change in peak shifts of the molecules is presented by solid arrows; dashed arrows demonstrate the peaks of the free species.

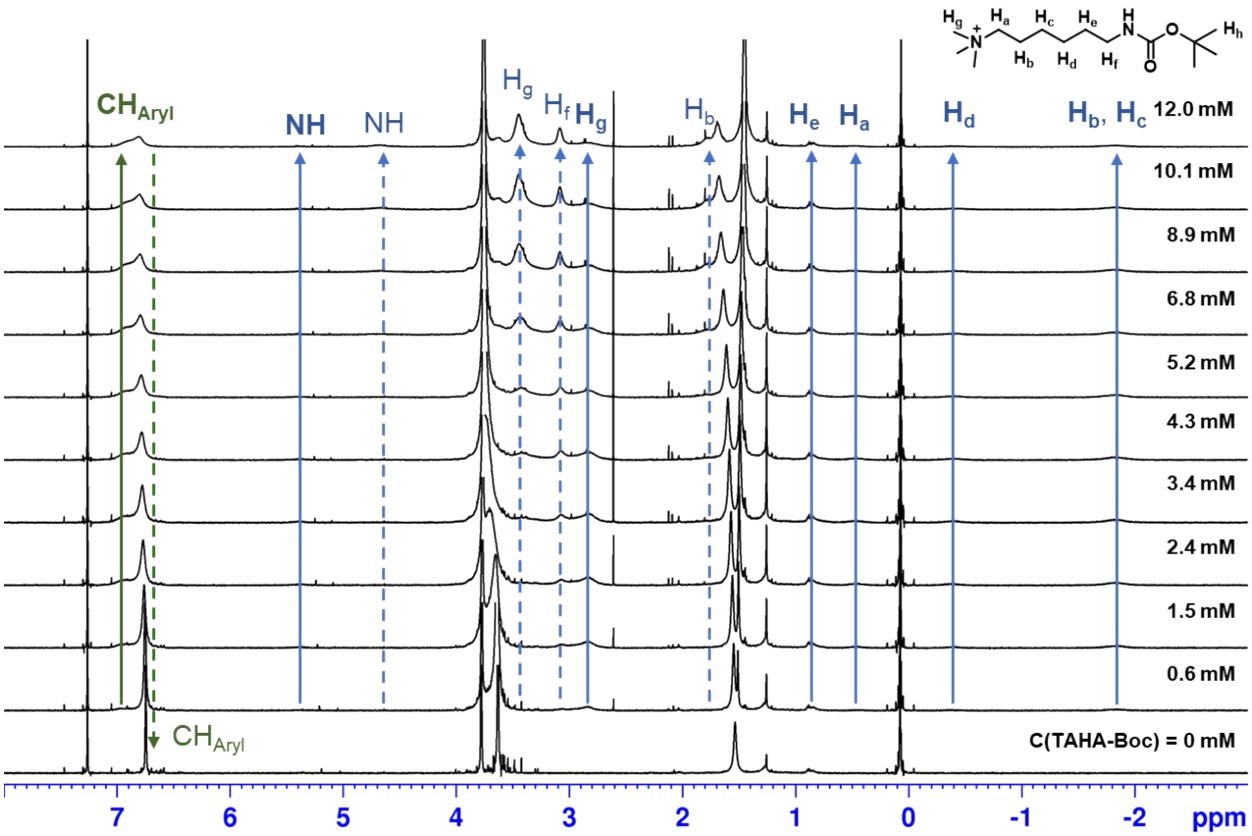

Figure S55. NMR titration of P5A with TAHA-Boc in $CDCl_3$ ($[H]_0$ = 4 mM). Normal and bold designations refer to free and complexed species.

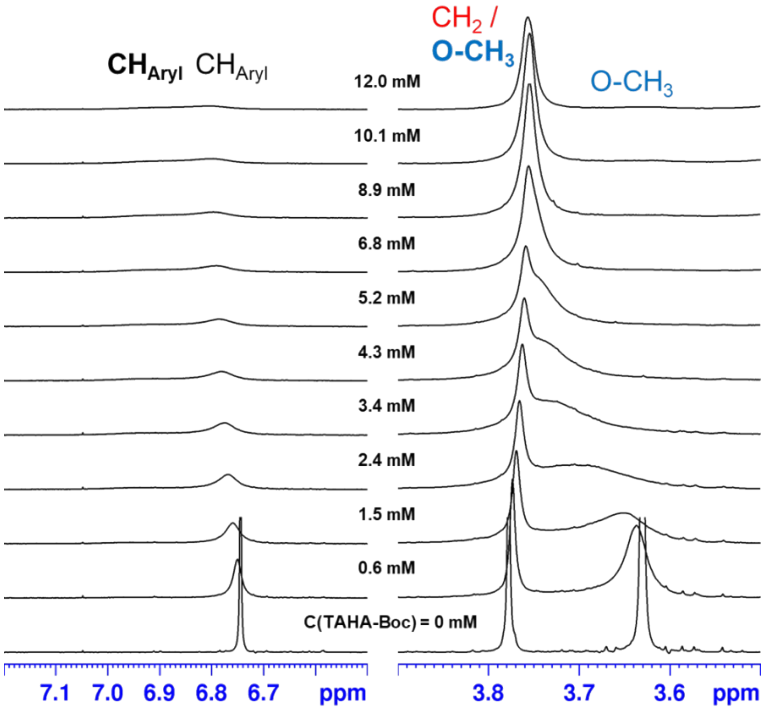

Figure S56. Fragments of the NMR titration (TAHA-Boc@P5A), with shifts of only P5A peaks shown.

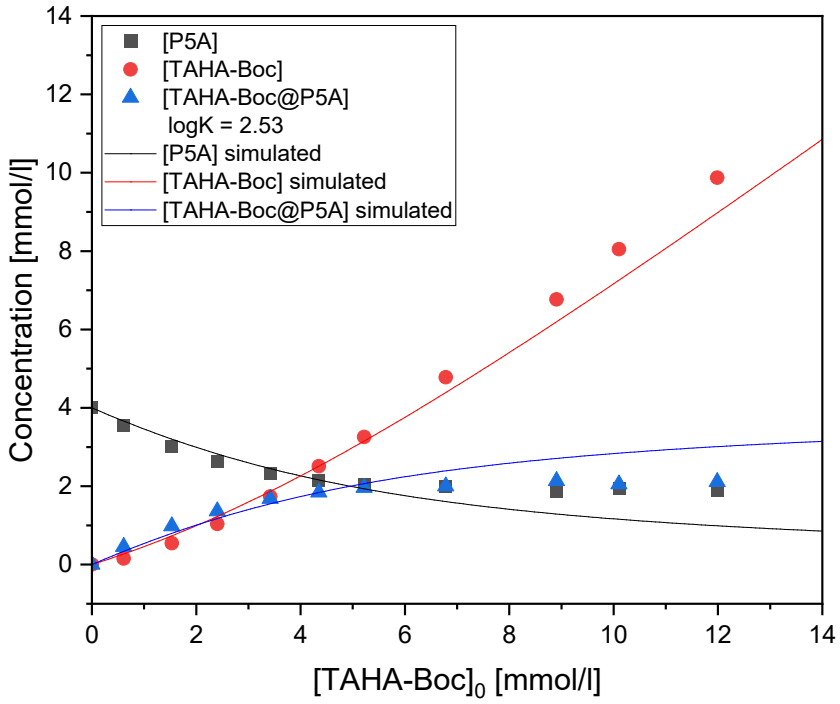

Figure S57. Titration curves for P5A–TAHA-Boc system. Scattered plots: experimental data, line plots: simulated (HySS 2009 software) curves. Calculated assuming 1:1 (host : guest) stoichiometry of the complex with log K_a = 2.53.

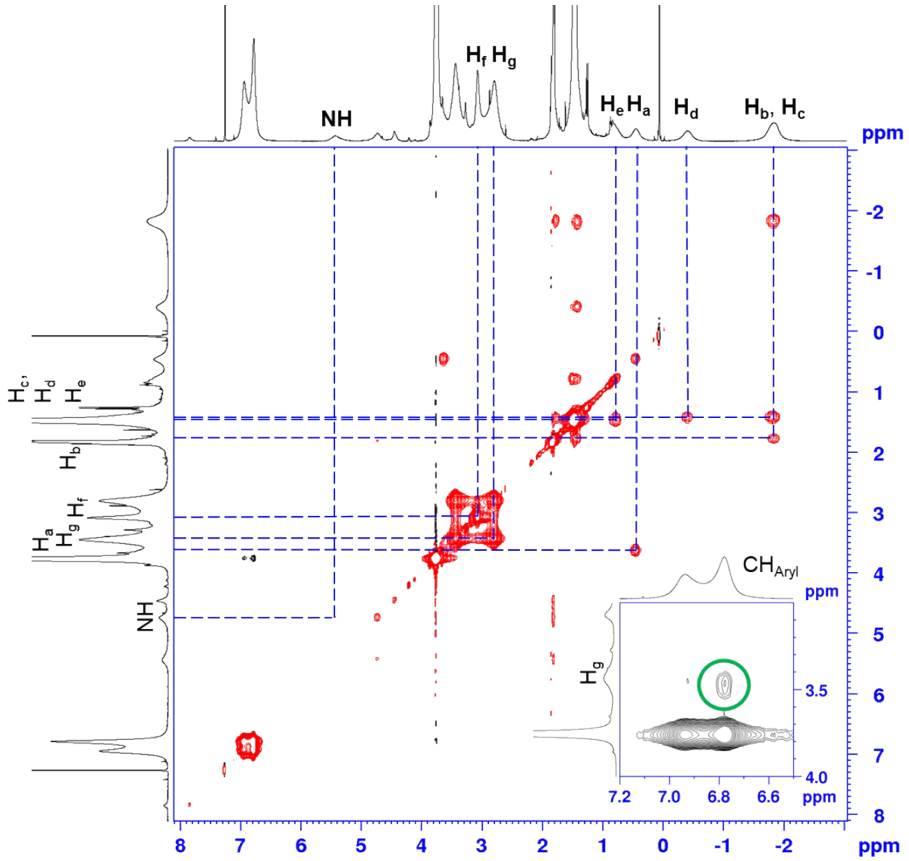

Figure S58. 2D NOESY NMR of the complex TAHA-Boc@P5A. The blue dashed lines represent the relation between the peaks of the free and bound guest. On the horizontal and vertical projections, the peaks of a bound and free (respectively) guest are marked. Inset: The NOE cross-peak between host and guest species is marked green.

Polymer characterization

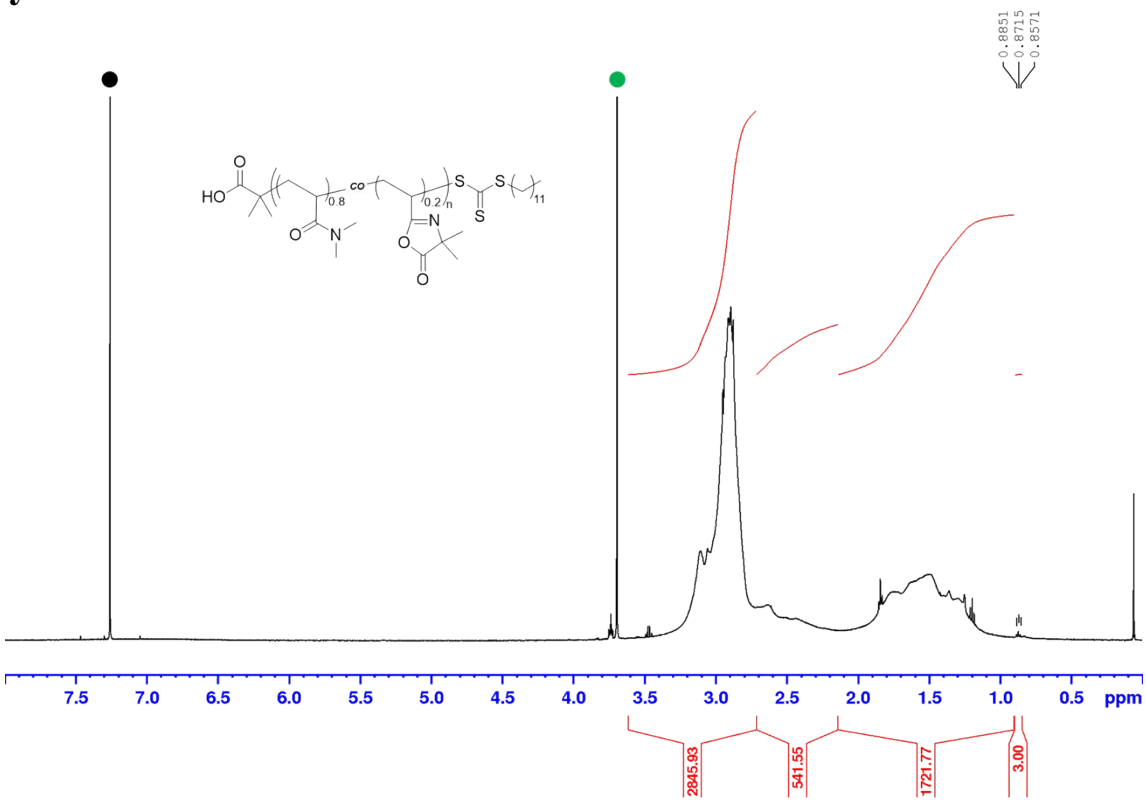

Figure S59. [1]H NMR spectrum of poly(DMAAm-co-VDMA) in $CDCl_3$.

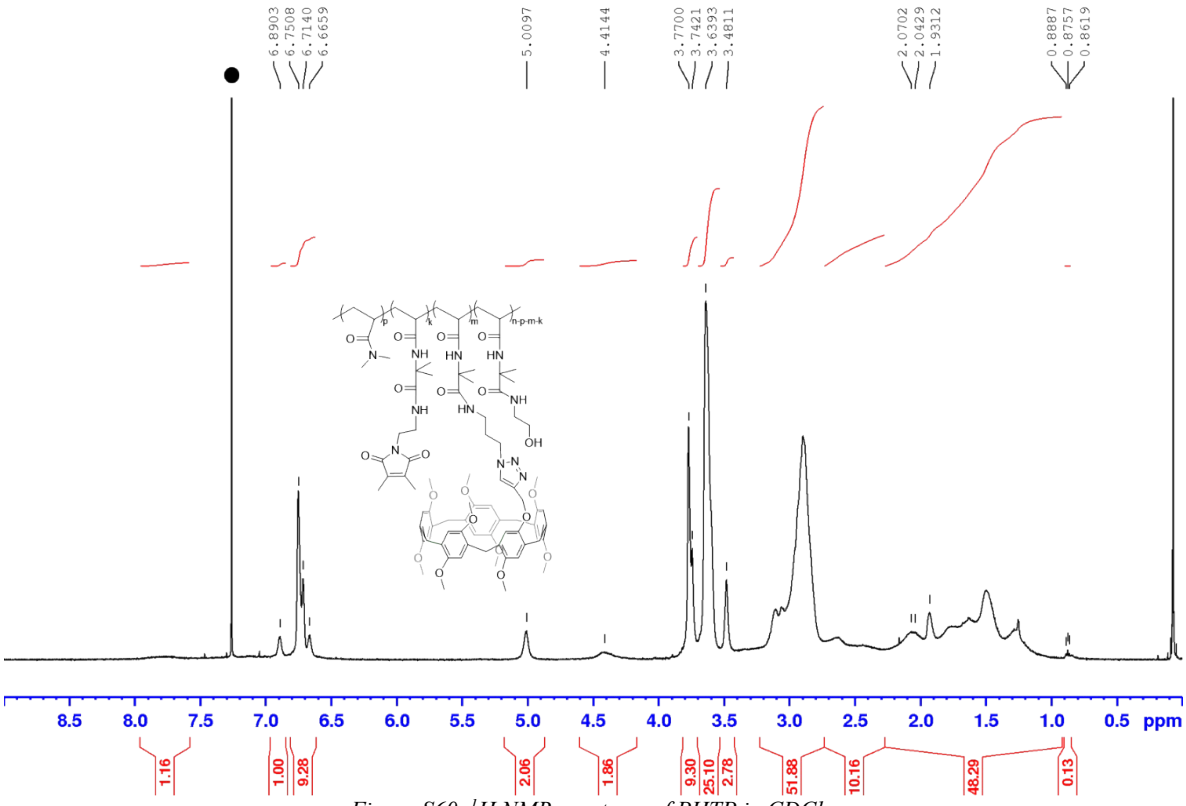

Figure S60. [1]H NMR spectrum of PHTP in $CDCl_3$.

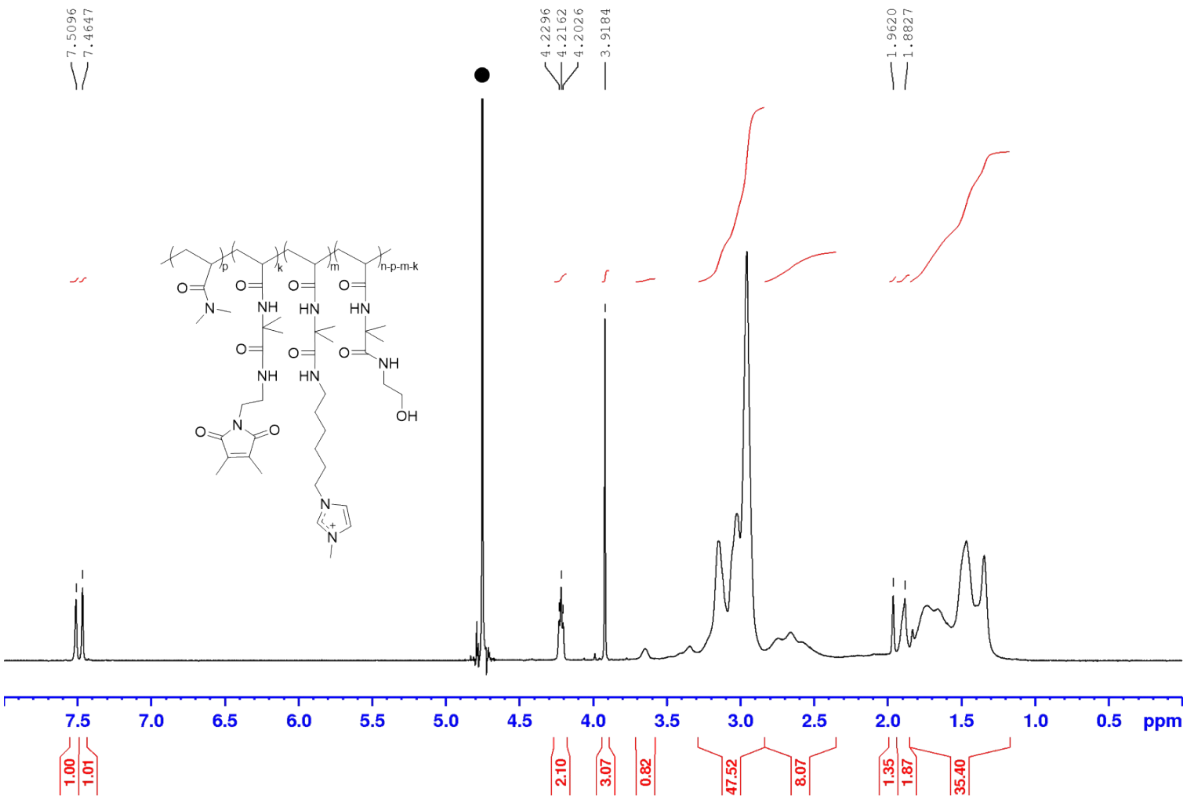

Figure S61. ^{1}H NMR spectrum of PMIHAP in D_2O.

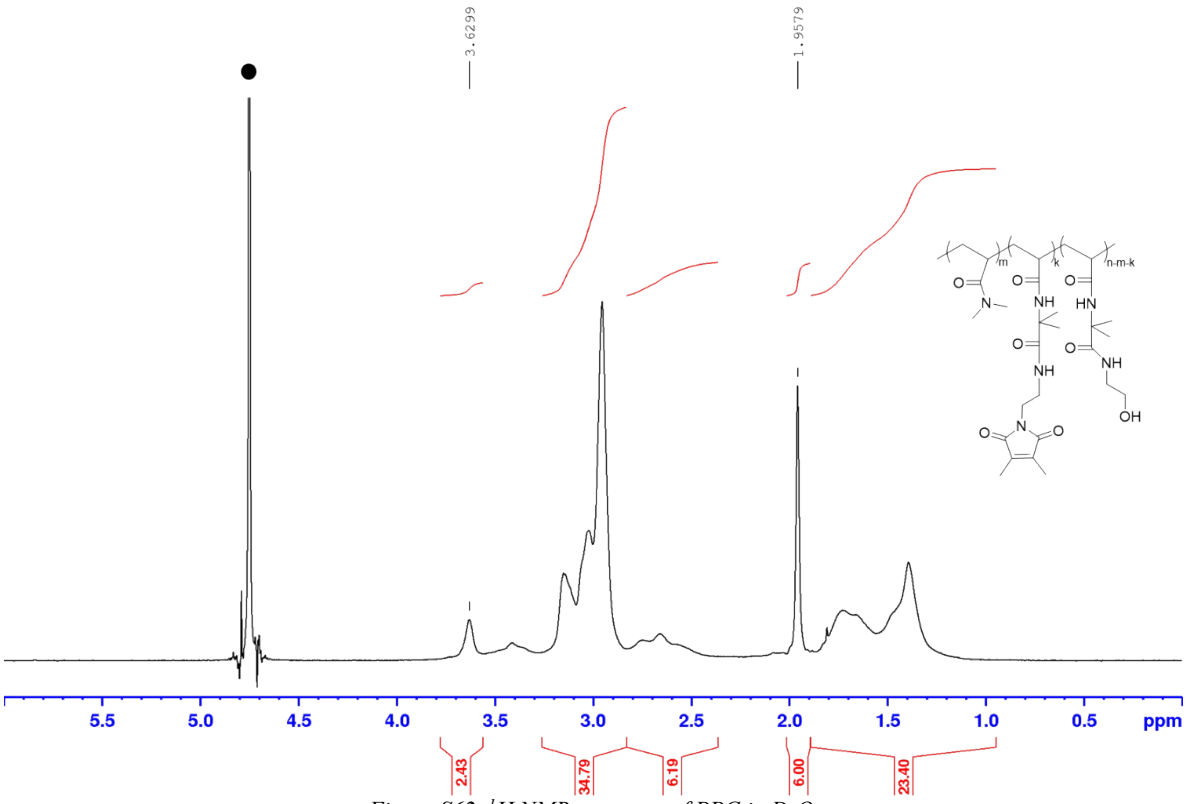

Figure S62. ^{1}H NMR spectrum of PPC in D_2O.

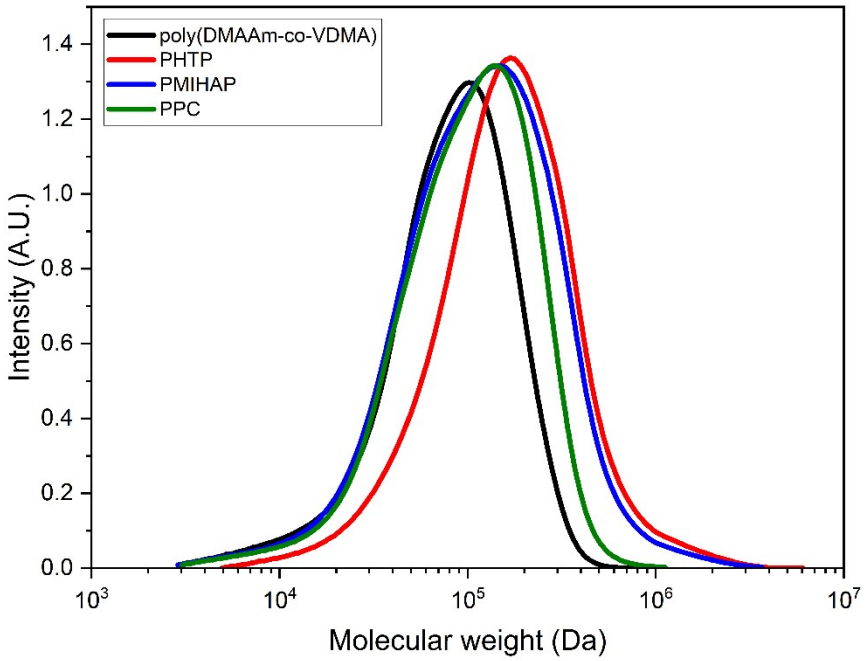

Figure S63. GPC elugrams (eluent: HFIP + 0.05 M CF_3COOK, PMMA calibration, BHT as internal standard) of the synthesized polymers: poly(DMAAm-co-VDMA), PHTP, PMIHAP and PPC.

SPR measurements

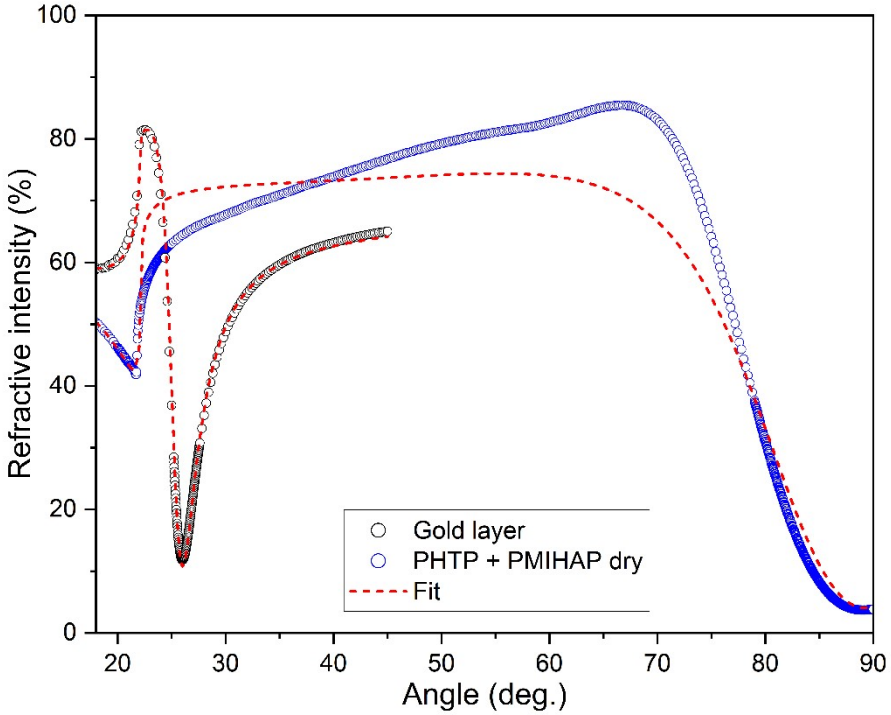

Figure S64. SPR scan measurement of a gold-coated wafer (black circles), PHTP+PMIHAP gel in a dry state (blue circles) and the fit by Winspall software (red dashed lines).

Table S2. Parameters of the polymeric gel sensor in different mediums

Medium	d^{in}, nm	d^{out}, nm	d, nm	Swelling ratio Q	n^{in}	n^{out}	Refractive index n_D
Gold layer			33.92				–11.6448 (ε') 1.3854 (ε'')
Air	–	–	187.2	–			1.5595
$CHCl_3$	269.6	482.7	752.4	4.02	1.4998	1.4771	1.4853
AN 1 μM	269.2	489.9	759.1	4.06	1.5000	1.4765	1.4848
AN 5 μM	267.6	491.3	758.9	4.05	1.5002	1.4764	1.4848
AN 10 μM	262.5	500.3	762.8	4.07	1.5000	1.4762	1.4844
AN 20 μM	266.2	497.7	763.9	4.08	1.4998	1.4760	1.4843
AN 50 μM	271.2	501.0	772.2	4.12	1.4998	1.4754	1.4840
AN 100 μM	272.5	507.1	779.6	4.16	1.4999	1.4749	1.4836
AN 200 μM	269.6	515.8	785.4	4.20	1.4996	1.4745	1.4831
AN 500 μM	262.3	543.5	805.8	4.30	1.4988	1.4732	1.4815
AN 1 mM	262.6	557.9	820.5	4.38	1.4987	1.4723	1.4808

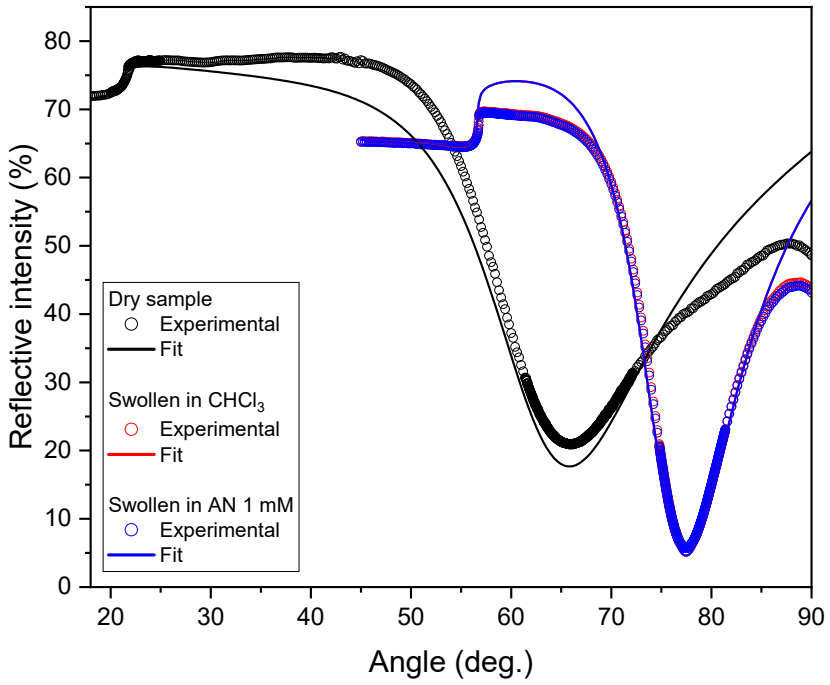

Figure S65. SPR curves of the PPC gel: dry (medium: air; black curves), swollen in $CHCl_3$ (red curves) and in 1 mM AN solution (blue curves).

Table S3. Parameters of the PPC gel in different mediums.

Medium	Gel thickness d, nm	Swelling ratio Q	Refractive index n_D
Air	122.0	–	1.4750
$CHCl_3$	461.6	3.78	1.4732
AN 1 mM	457.8	3.75	1.4738

Table S4. Parameters for the calculation of the LoD[S10]

AN concentration (μM)	$(Q_i - Q_{r,i})^2$	n	$s_{y/x}$	Slope A (μM^{-1})	LoD (μM)
1	9.99E-06	6	0.00851	0.00113	24.86
5	8.24E-05				
10	3.98E-05				
20	4.23E-07				
50	1.23E-04				
100	3.39E-05				

References

S1 J. Henig, I. Mamedov, P. Fouskova, É. Tóth, N. K. Logothetis, G. Angelovski and H. A. Mayer, *Inorg. Chem.*, 2011, **50**, 6472–6481.

S2 S. K. V. Vernekar, H. Y. Hallaq, G. Clarkson, A. J. Thompson, L. Silvestri, S. C. R. Lummis and M. Lochner, *J. Med. Chem.*, 2010, **53**, 2324–2328.

S3 K. Kai, H. Fujii, R. Ikenaka, M. Akagawa and H. Hayashi, *Chem. Commun.*, 2014, **50**, 8586–8589.
S4 A. Müller and P. Krauss, *Monatshefte für Chemie*, 1932, **61**, 219–228.
S5 M. E. Levere, H. T. Ho, S. Pascual and L. Fontaine, *Polym. Chem.*, 2011, **2**, 2878.
S6 X. Yu, A. Herberg and D. Kuckling, *Eur. Polym. J.*, 2019, **120**, 109207.
S7 S. M. Heilmann, K. M. Jensen, L. R. Krepski, D. M. Moren, J. K. Rasmussen and H. K. Smith, *Synth. Commun.*, 1987, **17**, 843–862.
S8 J. Li, X. Yu, A. Herberg and D. Kuckling, *Macromol. Rapid Commun.*, 2019, **40**, e1800674.
S9 C. D. Vo, D. Kuckling, H.-J. P. Adler and M. Schönhoff, *Colloid Polym. Sci.*, 2002, **280**, 400–409.
S10 D. J. Anderson, *Clin. Chem.*, 1989, **35**, 2152–2153.